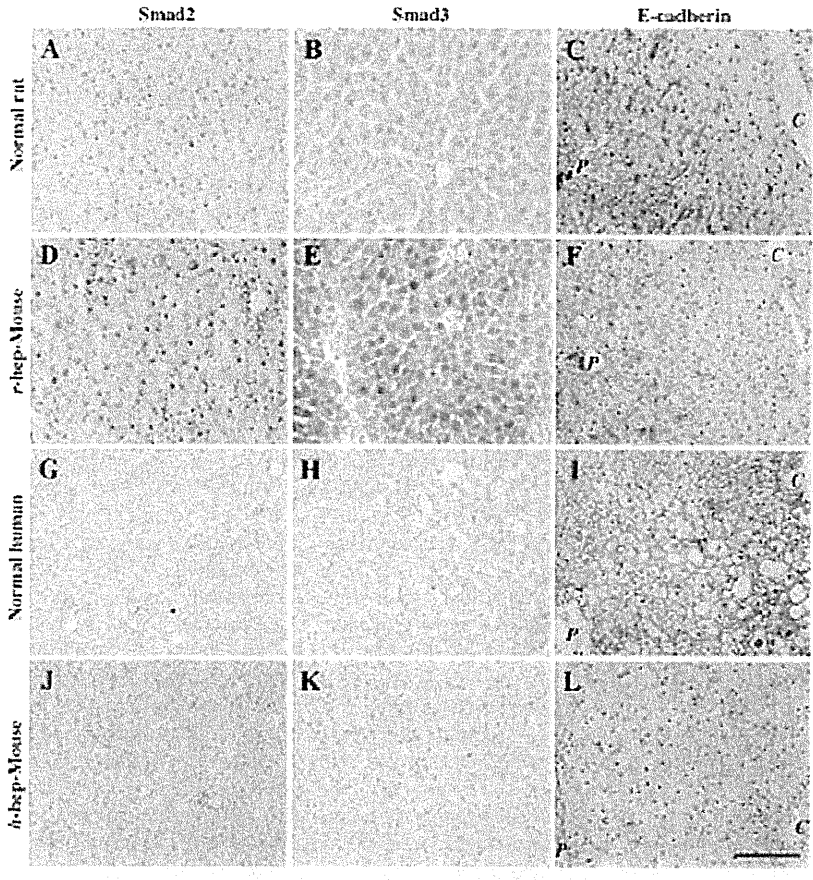

Figure 8. Localization of Smad2/3 and E-cadherin in chimeric mouse liver. Livers were obtained from 13-week-old male Fischer 344 rats (**A–C**, Normal rat), normal donors (49YM, 50YM, and 65YF) (**G–I**, Normal human), r-hep-mice at three weeks (**D** and **E**) and five weeks (**F**), and 9MM-h-hep-mice at 11 weeks (**J** and **K**) and 14 weeks (**L**) after transplantation. They were immunostained for Smad2 (**A**, **D**, **G**, and **J**), Smad3 (**B**, **E**, **H**, and **K**), and E-cadherin (**C**, **F**, **I**, and **L**). Positive signals are brown. Histological examinations were individually performed for these livers in each category, and we obtained similar results. Representative photos are shown here. The photos of Normal human were from 49YM liver. In **C**, **F**, **I**, and **L**, *P* and *C* indicate portal and central veins, respectively. Scale bar = 100 μm.

TGF-β and activin signaling was lacking in h-hep-mice. In h-hep mice from another donor (10YF, 9 to 11 weeks after transplantation), the immunohistological results for TGF-β, Smad2, and Smad3 showed the same tendencies as the results shown in Figures 7 and 8 (data not shown), suggesting that the deficiency of TGF-β signaling is not attributed to the possible immaturity because of the young age (9MM) of the donor.

To obtain an additional evidence for the TGF-β signaling deficiency in h-hep-mice, we examined the expression of E-cadherin in the chimeric mouse, which is one of the TGF-β target genes.[30] Normal r-livers expressed the E-cadherin protein in the periportal zone restrictedly (Figure 8C), and a similar distribution pattern was observed in the r-hep-mouse livers (Figure 8F). In contrast to normal r-livers, normal h-livers uniformly and evenly expressed E-cadherin (Figure 8I). Its expression was significantly low in the h-hepatocyte region of the h-hep-mouse liver (Figure 8I) compared with that in the normal h-livers.

Participation of m-HSCs in the Donor Hepatocyte Colonies

As shown in Figure 7, the xenogeneic hepatocyte regions contained fewer m-HSCs than the injured host regions, especially in the proliferation phase. We further investigated this phenomenon using desmin as a HSC marker. The desmin$^+$ cells were scarce in both r- and h-hepatocyte colonies in r-hep-mice at 2 weeks (Figure 9A) and in h-hep-mice at 5 weeks after transplantation (Figure 9B), respectively, compared with the degenerating m-hepatocyte regions that surrounded the corresponding donor cell regions. These xenogeneic hepatocytes were both in the proliferation phase (Figure 1). This paucity of HSCs seemed to be related to the fact that the sinusoids were still under reconstruction (Figure 4E) in r-hep-mouse liver at 2 weeks and in h-hep-mouse liver at 5 weeks (data not shown). HSCs were abundant in r-hepatocyte colonies in r-hep-mice at 3 weeks (termination phase) (Figure 9C), supporting the result of Figure 7J. The HSCs also increased in density in h-hepatocyte colonies of h-hep-mice at 11 weeks (Figure 9D), also supporting the result of Figure 7P. However, the density was apparently lower than that in r-hepatocyte colonies, most probably reflecting the fact that the sinusoids were less developed than in r-hepatocyte colonies in the termination phase (Figure 4N versus Figure 4H, respectively). These desmin$^+$ HSCs were not derived from h-HSCs, because, first the purity of the transplanted h-hepatocytes was >99% and second h-HSCs do not express desmin.[31] The m-HSC-occupied areas (red-colored areas) were measured in the entire normal mouse (wild-type SCID mouse) liver (control) and in the xenogeneic hepatocyte regions of chimeric livers on immunostained sections. The ratios (R_{HSC}) of red-colored areas

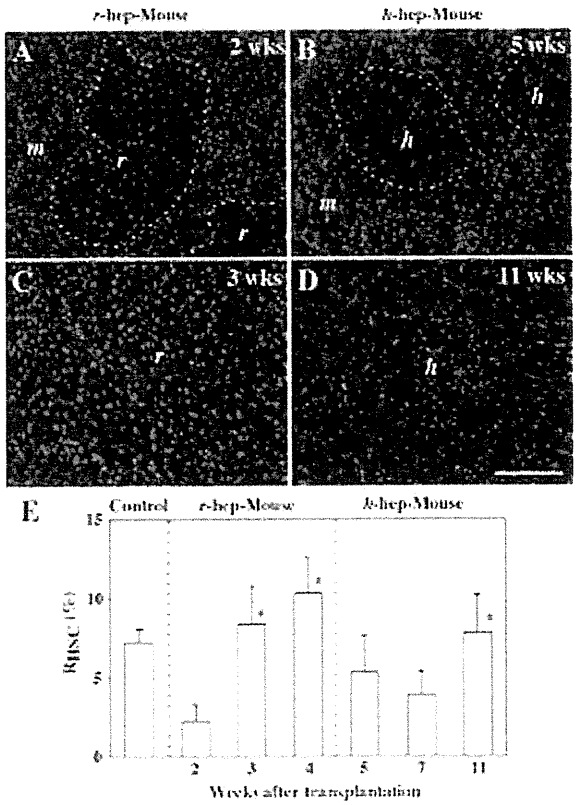

Figure 9. Distribution of m-HSCs in r- and h-hep-mice. Liver sections from r-hep-mice at two (proliferation phase, **A**) and three (termination phase, **C**) weeks and from 9MM h-hep-mice at five (proliferation phase, **B**) and 11 (termination phase, **D**) weeks after transplantation were immunostained for desmin (red). The nuclei were stained with Hoechst 33258 (blue). Serial sections from the r-hep- and h-hep-mouse livers were immunostained for rRT1A and hCK8/18 to identify r-and h-hepatocytes, respectively (data not shown), from which the boundary between the host (*m*) and transplanted (*r* or *h*) hepatocyte regions was determined, as indicated by the **dashed lines** in **A** and **B**. Similar results were obtained from three different mice. Scale bar = 100 μm. **E:** Changes in the ratio of desmin$^+$ cells in xenogeneic hepatocyte regions during liver repopulation. Liver sections from 3-month-old wild-type SCID mice (control), r- and h-hep-mice at the indicated weeks after transplantation were immunostained for desmin. Serial sections were stained with anti-rRT1A and -hCK8/18 antibodies to identify r- and h-hepatocytes, respectively. The ratio (R_{HSC}) of desmin$^+$ areas over the measured areas was calculated in the xenogeneic hepatocyte region using NIH imaging software and is expressed as a percentage. Data represent the mean ± SD of desmin$^+$ area per section in a total of 15 randomly selected fields ($n = 3$). **Asterisks** at three and four weeks in the panel for r-hep-mice indicate significant differences versus the value at two weeks. The **asterisk** at 11 weeks in the panel of h-hep-mice indicates a significant difference versus the value at five weeks.

to either the entire liver of SCID mouse or to the xenogeneic region of chimeric liver were calculated and are shown in Figure 9E. The R_{HSC} in normal mice was 7.3 ± 0.8%. In r-hep-mice, the R_{HSC} was 2.3 ± 1.1% at 2 weeks and increased to 10.3 ± 2.3% at 4 weeks. In h-hep-mice, the R_{HSC} was approximately 5% for up to 7 weeks and significantly increased to 7.8 ± 2.4% ($P < 0.01$) at 11 weeks. The R_{HSC} of r-hep-mice at 4 weeks was significantly higher than that of h-hep-mice at 11 weeks ($P < 0.01$).

Discussion

In this study, we compared the repopulation processes between r- and h-hepatocytes in the livers of uPA/SCID mice and showed several physiologically significant differences. The r-hepatocytes rapidly replaced m-hepatocytes to keep a normal $R_{L/B}$, suggesting a repopulation in a strictly regulated manner. The r-hepatocytes expressed TGFBR1/2 mRNAs at lower levels in the proliferation phase and then gradually increased expressions in the termination phase when m-HSCs actively expressed TGF-β. Moreover, Smad2/3 were translocated in r-hepatocyte nuclei, suggesting that TGF-β/TGFBR/Smad signaling normally works as in the terminal phase of mouse liver regeneration.

In the chimeric animal h-hepatocytes were quite different from r-hepatocytes. They proliferated much slowly, requiring approximately four times longer to complete proliferation than r-hepatocytes. The resulting liver showed marked overgrowth compared with a normal m-liver. TGFBR2 and ACVR2A, and TGF-β were not up-regulated in h-hepatocytes and m-HSCs of h-hep-mice, respectively, in the termination phase, indicating the absence of physiologically meaningful signaling between h-hepatocytes and m-HSCs. The density of m-HSCs in h-hepatocyte colonies was lower than that in r-hepatocyte colonies even in the termination phase, which probably reflects the poor development of sinusoids in h-hep-mice, because the multiple hepatic plates would result in the lower volume of the space of Disse than in the liver with single hepatic plates. It has been reported that intimate signaling between hepatocytes and nonparenchymal cells plays an important role in the termination of liver regeneration.[32] Thus, the failure of m-HSCs to express TGF-β could be a cause of liver hyperplasia of h-hep-mice. However, it is appropriate to note here that other factors such as hepatocyte growth factor[33] and bile acids[34] might be involved in the observed hyperplasia.

In TGFBR2 knockout mice, partial hepatectomy resulted in a 1.2-fold increase beyond the normal liver weight because of a compensatory increase in activin A/ACVR2A signaling and persistent activity in the Smad pathway.[20] Unlike in the study cited, the levels of ACVR2A mRNA and Smad proteins remained low through the experimental period in the present study with h-hep-mice. Thus, the lack of both TGF-β and activin signaling may have been partly responsible for the observed overgrowth of hepatocytes. We did not observe any symptoms of carcinogenic transformation in h-hepatocytes (data not shown), although TGFBR2[35] and ACVR2[36] are putative tumor suppressors, suggesting a requirement for additional factor(s) for hepatocarcinogenesis.

Even in the absence of TGF-β/TGFBR signaling, the transplanted h-hepatocytes eventually terminated proliferation. The histological features of sinusoids and canaliculi in mouse liver repopulated by xenogeneic hepatocytes demonstrated that h-hepatocytes did not restore the normal arrangement of single hepatic plates in the resting phase of the liver, but they formed multiple hepatic plates seen in the regenerating liver.[25,26] Thus, it is most likely that h-hepatocytes eventually terminated the proliferation because of contact inhibition within the multiple hepatocyte layers. r-Hepatocytes also formed multiple hepatic plates in the proliferation phase but restored the normal structures of single cell plates along the portal-central axis in the termination phase. It seems that

TGF-β/TGFBR signaling is required for both the formation of single hepatic plates and the normal termination of liver growth. These apparently distinct events (liver growth termination and hepatic plate structuring) should be closely related at the molecular levels, because adhesion molecules such as E-cadherin and β1-integrin are reported as the Smad2/3-mediated TGF-β target genes in liver development.[30] Our results demonstrated that E-cadherin uniformly exists on the hepatocyte surfaces in the normal h-liver, but its expression was quite low in substantial portions of the h-hepatocyte region in the h-hep-mouse liver. It is likely that this expression defect in the cell adhesion molecule results in abnormal hepatocyte plate arrangements. Loss of TGF-β signaling in h-hep-mice might be responsible for the maintenance of multicell-thick hepatic plates after the termination of liver repopulation in the h-hep-mouse livers.

There is the possibility that the observed hyperplasia of h-hepatocytes is the result of a signaling failure between m-cytokine ligands and the corresponding h-receptors. Recently, we showed that h-hepatocytes in h-hep-mice are growth hormone-deficient, because mouse growth hormone does not recognize the human growth hormone receptor of h-hepatocytes.[37] However, we consider that h-hepatocytes would be able to respond to TGF-β if the host m-HSCs secreted it, because there has been no report of species specificity between h- and m-TGF-β. In the present study we clearly demonstrated the coincidence of lack of TGF-β/TGFBR signaling with the hyperplasia of h-hep-mouse liver. However, the direct causality between such signaling and the liver hyperplasia remains to be examined. It is well known that hepatocytes and stellate cells interact with each other through varieties of signaling molecules and together contribute to physiological and pathological changes of liver. Therefore, we conclude that the lack of or weak interaction between h-hepatocytes and m-HSCs, which we have revealed at the histological and gene/protein expression levels, is responsible for the presently observed hyperplasia of h-hep-mouse liver.

Xenotransplantation, such as from pigs to humans, could potentially compensate for the lack of human organ and tissue donors. Our results indicate that, in addition to potential immunological rejection, the transplanted cells or tissues may fail to interact appropriately with the host environment. We propose that the h-chimeric mouse is a useful model for not only examining the mechanism of liver regeneration but also studying risks of xenotransplantation.

Acknowledgments

We thank Yasumi Yoshizane, Hiromi Kohno, Yoko Matsumoto, and Sanae Nagai for technical assistance and Dr. Masumi Yamada for helpful discussion and comments.

References

1. Heckel JL, Sandgren EP, Degen JL, Palmiter RD, Brinster RL: Neonatal bleeding in transgenic mice expressing urokinase-type plasminogen activator. Cell 1990, 62:447–456
2. Locaputo S, Carrick TL, Bezerra JA: Zonal regulation of gene expression during liver regeneration of urokinase transgenic mice. Hepatology 1999, 29:1106–1113
3. Rhim JA, Sandgren EP, Degen JL, Palmiter RD, Brinster RL: Replacement of diseased mouse liver by hepatic cell transplantation. Science 1994, 263:1149–1152
4. Rhim JA, Sandgren EP, Palmiter RD, Brinster RL: Complete reconstitution of mouse liver with xenogeneic hepatocytes. Proc Natl Acad Sci USA 1995, 92:4942–4946
5. Dandri M, Burda MR, Gocht A, Török E, Pollok JM, Rogler CE, Will H, Petersen J: Woodchuck hepatocytes remain permissive for hepadnavirus infection and mouse liver repopulation after cryopreservation. Hepatology 2001, 34:824–833
6. Dandri M, Burda MR, Török E, Pollok JM, Iwanska A, Sommer G, Rogiers X, Rogler CE, Gupta S, Will H, Greten H, Petersen J: Repopulation of mouse liver with human hepatocytes and in vivo infection with hepatitis B virus. Hepatology 2001, 33:981–988
7. Tateno C, Yoshizane Y, Saito N, Kataoka M, Utoh R, Yamasaki C, Tachibana A, Soeno Y, Asahina K, Hino H, Asahara T, Yokoi T, Furukawa T, Yoshizato K: Near completely humanized liver in mice shows human-type metabolic responses to drugs. Am J Pathol 2004, 165:901–912
8. Meuleman P, Libbrecht L, De Vos R, de Hemptinne B, Gevaert K, Vandekerckhove J, Roskams T, Leroux-Roels G: Morphological and biochemical characterization of a human liver in an uPA-SCID mouse chimera. Hepatology 2005, 41:847–856
9. Emoto K, Tateno C, Hino H, Amano H, Imaoka Y, Asahina K, Asahara T, Yoshizato K: Efficient in vivo xenogeneic retroviral vector-mediated gene transduction into human hepatocytes. Hum Gene Ther 2005, 16:1168–1674
10. Kam I, Lynch S, Svanas G, Todo S, Polimeno L, Francavilla A, Penkrot RJ, Takaya S, Ericzon BG, Starzl TE, Van Thiel DH: Evidence that host size determines liver size: studies in dogs receiving orthotopic liver transplants. Hepatology 1987, 7:362–366
11. Van Thiel DH, Gavaler JS, Kam I, Francavilla A, Polimeno L, Schade RR, Smith J, Diven W, Penkrot RJ, Starzl TE: Rapid growth of an intact human liver transplanted into a recipient larger than the donor. Gastroenterology 1987, 93:1414–1419
12. Francavilla A, Zeng Q, Polimeno L, Carr BI, Sun D, Porter KA, Van Thiel DH, Starzl TE: Small-for-size liver transplantation into large recipient: a model of hepatic regeneration. Hepatology 1994, 19:210–216
13. Nakamura T, Tomita Y, Hirai R, Yamaoka K, Kaji K, Ichihara A: Inhibitory effect of transforming growth factor-β on DNA synthesis of adult rat hepatocytes in primary culture. Biochem Biophys Res Commun 1985, 133:1042–1050
14. Russell WE, Coffey RJ Jr., Ouellette AJ, Moses HL: Type β transforming growth factor reversibly inhibits the early proliferative response to partial hepatectomy in the rat. Proc Natl Acad Sci USA 1988, 85:5126–5130
15. Zhang YQ, Kanzaki M, Mashima H, Mine T, Kojima I: Norepinephrine reverses the effects of activin A on DNA synthesis and apoptosis in cultured rat hepatocytes. Hepatology 1996, 23:288–293
16. Hu PP, Datto MB, Wang XF: Molecular mechanisms of transforming growth factor-β signaling. Endocr Rev 1998, 19:349–363
17. Kumar A, Novoselov V, Celeste AJ, Wolfman NM, ten Dijke P, Kuehn MR: Nodal signaling uses activin and transforming growth factor-β receptor-regulated Smads. J Biol Chem 2001, 276:656–661
18. Braun L, Mead JE, Panzica M, Mikumo R, Bell GI, Fausto N: Transforming growth factor β mRNA increases during liver regeneration: a possible paracrine mechanism of growth regulation. Proc Natl Acad Sci USA 1988, 85:1539–1543
19. Romero-Gallo J, Sozmen EG, Chytil A, Russell WE, Whitehead R, Parks WT, Holdren MS, Her MF, Gautam S, Magnuson M, Moses HL, Grady WM: Inactivation of TGF-β signaling in hepatocytes results in an increased proliferative response after partial hepatectomy. Oncogene 2005, 24:3028–3041
20. Oe S, Lemmer ER, Conner EA, Factor VM, Levéen P, Larsson J, Karlsson S, Thorgeirsson SS: Intact signaling by transforming growth factor β is not required for termination of liver regeneration in mice. Hepatology 2004, 40:1098–1105
21. Hino H, Tateno C, Sato H, Yamasaki C, Katayama S, Kohashi T, Aratani A, Asahara T, Dohi K, Yoshizato K: A long-term culture of human hepatocytes which show a high growth potential and express

their differentiated phenotypes. Biochem Biophys Res Commun 1999, 256:184–191
22. Seglen PO: Preparation of isolated rat liver cells. Methods Cell Biol 1976, 13:29–83
23. Utoh R, Tateno C, Yamasaki C, Hiraga N, Kataoka M, Shimada T, Chayama K, Yoshizato K: Susceptibility of chimeric mice with livers repopulated by serially subcultured human hepatocytes to hepatitis B virus. Hepatology 2008, 47:435–446
24. Livak KJ, Schmittgen TD: Analysis of relative gene expression data using real-time quantitative PCR and the $2^{-\Delta\Delta C_T}$ method. Methods 2001, 25:402–408
25. Wack KE, Ross MA, Zegarra V, Sysko LR, Watkins SC, Stolz DB: Sinusoidal ultrastructure evaluated during the revascularization of regenerating rat liver. Hepatology 2001, 33:363–378
26. Martinez-Hernandez A, Delgado FM, Amenta PS: The extracellular matrix in hepatic regeneration. Localization of collagen types I, III, IV, laminin, and fibronectin. Lab Invest 1991, 64:157–166
27. Keppler D, Konig J: Hepatic canalicular membrane 5: expression and localization of the conjugate export pump encoded by the MRP2 (cMRP/cMOAT) gene in liver. FASEB J 1997, 11:509–516
28. Michalopoulos GK: Liver regeneration. J Cell Physiol 2007, 213: 286–300
29. Chari RS, Price DT, Sue SR, Meyers WC, Jirtle RL: Down-regulation of transforming growth factor beta receptor type I, II, and III during liver regeneration. Am J Surg 1995, 169:126–132
30. Weinstein M, Monga SP, Liu Y, Brodie SG, Tang Y, Li C, Mishra L, Deng CX: Smad proteins and hepatocyte growth factor control parallel regulatory pathways that converge on β1-integrin to promote normal liver development. Mol Cell Biol 2001, 21:5122–5131
31. Cassiman D, Libbrecht L, Desmet V, Denef C, Roskams T: Hepatic stellate cell/myofibroblast subpopulations in fibrotic human and rat livers. J Hepatol 2002, 36:200–209
32. Koniaris LG, McKillop IH, Schwartz SI, Zimmers TA: Liver regeneration. J Am Coll Surg 2003, 197:634–659
33. Patijn GA, Lieber A, Schowalter DB, Schwall R, Kay MA: Hepatocyte growth factor induces hepatocyte proliferation in vivo and allows for efficient retroviral-mediated gene transfer in mice. Hepatology 1998, 28:707–716
34. Huang W, Ma K, Zhang J, Qatanani M, Cuvillier J, Liu J, Dong B, Huang X, Moore DD: Nuclear receptor–dependent bile acid signaling is required for normal liver regeneration. Science 2006, 312:233–236
35. Derynck R, Akhurst RJ, Balmain A: TGF-β signaling in tumor suppression and cancer progression. Nat Genet 2001, 29:117–129
36. Jeruss JS, Sturgis CD, Rademaker AW, Woodruff TK: Down-regulation of activin, activin receptors, and Smads in high-grade breast cancer. Cancer Res 2003, 63:3783–3790
37. Masumoto N, Tateno C, Tachibana A, Utoh R, Morikawa Y, Shimada T, Momisako H, Itamoto T, Asahara T, Yoshizato K: GH enhances proliferation of human hepatocytes grafted into immunodeficient mice with damaged liver. J Endocrinol 2007, 194:529–553

Supplemental Material can be found at:
http://dmd.aspetjournals.org/content/suppl/2010/08/06/dmd.109.031732.DC1.html

0090-9556/10/3811-1954–1961$20.00
DRUG METABOLISM AND DISPOSITION
Vol. 38, No. 11
31732/3633215
Printed in U.S.A.
Copyright © 2010 by The American Society for Pharmacology and Experimental Therapeutics
DMD 38:1954–1961, 2010

Effect of Hepatitis C Virus Infection on the mRNA Expression of Drug Transporters and Cytochrome P450 Enzymes in Chimeric Mice with Humanized Liver[S]

Ryota Kikuchi, Matthew McCown, Pamela Olson, Chise Tateno, Yoshio Morikawa, Yumiko Katoh, David L. Bourdet, Mario Monshouwer, and Adrian J. Fretland

Non Clinical Safety, Department of Drug Metabolism and Pharmacokinetics (R.K., D.L.B., M.Mo., A.J.F.), Viral Disease Biology Area (M.Mc.), and Molecular Medicine Laboratories (P.O.), Roche Palo Alto, Palo Alto, California; and PhoenixBio Co., Ltd., Higashi-Hiroshima, Japan (C.T., Y.M., Y.K.)

Received December 16, 2009; accepted August 6, 2010

ABSTRACT:

The expression of drug transporters and metabolizing enzymes is a primary determinant of drug disposition. Chimeric mice with humanized liver, including PXB mice, are an available model that is permissive to the in vivo infection of hepatitis C virus (HCV), thus being a promising tool for investigational studies in development of new antiviral molecules. To investigate the potential of HCV infection to alter the pharmacokinetics of small molecule antiviral therapeutic agents in PXB mice, we have comprehensively determined the mRNA expression profiles of human ATP-binding cassette (ABC) transporters, solute carrier (SLC) transporters, and cytochrome P450 (P450) enzymes in the livers of these mice under noninfected and HCV-infected conditions. Infection of PXB mice with HCV resulted in an increase in the mRNA expression levels of a series of interferon-stimulated genes in the liver. For the majority of genes involved in drug disposition, minor differences in the mRNA expression of ABC and SLC transporters as well as P450s between the noninfected and HCV-infected groups were observed. The exceptions were statistically significantly higher expression of multidrug resistance-associated protein 4 and organic anion-transporting polypeptide 2B1 and lower expression of organic cation transporter 1 and CYP2D6 in HCV-infected mice. Furthermore, the enzymatic activities of the major human P450s were, in general, comparable in the two experimental groups. These data suggest that the pharmacokinetic properties of small molecule antiviral therapies in HCV-infected PXB mice are likely to be similar to those in noninfected PXB mice. However, caution is needed in the translation of this relationship to HCV-infected patients as the PXB mouse model does not accurately reflect the pathology of patients with chronic HCV infection.

Introduction

Elimination of endogenous and exogenous substances is one of the most important physiological functions of the liver, which comprises the sinusoidal uptake from the blood circulation, intracellular phase I and phase II metabolism, and canalicular efflux of parent compound and/or metabolites into bile. Cumulative evidence suggests that members of the solute carrier (SLC) and ATP-binding cassette (ABC) transporters are expressed on either sinusoidal or canalicular membrane of the hepatocytes where they are responsible for the sinusoidal uptake and bile canalicular efflux of a diverse set of compounds (Chandra and Brouwer, 2004; Shitara et al., 2006; Dobson and Kell, 2008). On the other hand, cytochrome P450 enzymes are localized to the endoplasmic reticulum of hepatocytes and are the major enzymes involved in phase I drug metabolism and bioactivation, accounting for approximately 75% of the oxidative metabolism of marketed drugs (Gonzalez, 1990; Rendic and Di Carlo, 1997). Other enzymes such as glutathione transferase, UDP-glucuronosyltransferase, and sulfotransferase are involved in the conjugation of xenobiotics in phase II metabolism (Meyer, 1996; Williams et al., 2004). The expression and function of these transporters and enzymes are important determinants of the physiological turnover of endogenous compounds and clearance of exogenous substances including clinically used drugs.

Hepatitis C virus (HCV) infects an estimated 170 million people worldwide, and its infection is a leading cause of chronic hepatitis, liver cirrhosis, and hepatocellular carcinoma (World Health Organization, 1999). Currently, the combination therapy of pegylated interferon (IFN) and ribavirin is the only approved treatment for HCV infection. However, this treatment regimen is only effective in ap-

Article, publication date, and citation information can be found at http://dmd.aspetjournals.org.
doi:10.1124/dmd.109.031732.
[S] The online version of this article (available at http://dmd.aspetjournals.org) contains supplemental material.

ABBREVIATIONS: SLC, solute carrier; ABC, ATP-binding cassette; HCV, hepatitis C virus; IFN, interferon; uPA/SCID, urokinase plasminogen activator-transgenic severe combined immunodeficiency disorder; PCR, polymerase chain reaction; ISG, interferon-stimulated gene; hGAPDH, human glyceraldehyde-3-phosphate dehydrogenase; P450, cytochrome P450; LC, liquid chromatography; MS/MS, tandem mass spectrometry; MRP, multidrug resistance-associated protein; OATP, organic anion-transporting polypeptide; OCT, organic cation transporter; P-gp, P-glycoprotein; MDR, multidrug resistance; BSEP, bile salt export pump; NTCP, Na^+-taurocholate cotransporting polypeptide; OAT, organic ion transporter; C_t, cycle threshold.

DRUG METABOLISM AND DISPOSITION DMD aspet

proximately 50% of all patients infected with HCV. A number of individuals with HCV infection are unable to achieve a sustained virological response with the current therapy, and many of them will progress to liver diseases resulting from chronic infection with HCV. Thus, the development of more efficient therapies against HCV is of high priority (Wakita, 2007).

Several in vitro experimental models have been used to investigate the pathology of HCV as well as the efficacy of potential therapeutic compounds. These models include the use of individually cloned proteins of HCV (Littlejohn et al., 1998), infection of primary culture human hepatocytes with HCV (Buck, 2008), and in vitro HCV replicon systems in Huh-7 cells (Bartenschlager, 2005). The HCV replicon systems are particularly useful in HCV research and drug discovery because they are both permissive to high-efficiency HCV replication and respond to antiviral compounds including IFN-α and ribavirin. However, several limitations exist with the use of replicon systems in the discovery and development of novel anti-HCV compounds. These include the cell culture-adaptive mutations of the HCV genome and the innate difference of Huh-7 cells, which are immortalized tumor cells, compared with hepatocytes.

Because of the strict tropism of HCV, only humans and higher primates, such as chimpanzees, have, until recently, been receptive to authentic HCV infection and the development of chronic liver disease due to HCV infection (Lanford et al., 2001; Kremsdorf and Brezillon, 2007). However, use of chimpanzees is difficult from ethical and economical perspectives. The chimeric mouse with a humanized liver on the genetic background of urokinase plasminogen activator-transgenic severe combined immunodeficiency disorder (uPA/SCID) mice, designated as the PXB mouse, has been developed and characterized (Tateno et al., 2004). The livers of these mice are near completely (>70%) replaced with human hepatocytes and maintain the hepatic expression of most human drug-metabolizing enzymes and transporters (Nishimura et al., 2005). Subsequent studies have demonstrated that this mouse model is permissive to the infection of HCV in vivo and has potential utility in the discovery and development of new anti-HCV therapy (Umehara et al., 2006; Hiraga et al., 2007; Inoue et al., 2007). However, one should note that HCV-infected PXB mice do not precisely mimic chronic HCV infection in humans because these mice lack the adaptive immune response and liver disease associated with HCV infection as a result of their genetic background (SCID).

Because the primary organ of HCV infection and its replication is the liver, it is of great importance to know the possible alterations in the hepatic expression and activity of pharmacokinetics-related genes, i.e., drug transporters and metabolizing enzymes, by HCV infection. The aim of the present study was thus to investigate the effect of HCV infection on the mRNA expression of human ABC and SLC transporters and cytochrome P450 enzymes in the livers of PXB mice. Furthermore, the enzymatic activities of major human cytochrome P450 enzymes were compared between noninfected and HCV-infected PXB mice.

Materials and Methods

Generation of PXB Mice. PXB mice were generated by transplanting 1.0×10^6 human hepatocytes into the spleens of 2- to 3-week-old uPA/SCID mice under diethyl ether anesthesia as described previously (Tateno et al., 2004). All PXB mice used in the present study were derived from the same donor human hepatocyte (BD87, male, 2-year-old white; BD Biosciences, San Jose, CA).

Inoculation of HCV to PXB Mice. The inoculum used in the present study was HCV genotype 1b (HCR6, accession no. AY045702), which was obtained from HCV-infected PXB mice at the third passage. The original inoculum was obtained from the serum of an HCV-positive patient. PXB mice with a human albumin concentration in the blood greater than 6.0 mg/ml were infected with HCV genotype 1b at 9 to 10 weeks of age by injecting the inoculum (1.0×10^4 copies/mouse) to the retro-orbital sinus under diethyl ether anesthesia.

Quantification of Human Albumin Concentration and HCV Titer in the Serum. The concentration of human albumin in mouse blood was determined by latex agglutination immunonephelometry at 13 to 17 weeks of age. The replacement index is defined as the percentage of human hepatocyte repopulated in the host mouse liver and can be estimated from the blood human albumin value. RNA was extracted from the serum of PXB mice using a Sepa Gene RV-R RNA extraction system (Sanko Junyaku Co., Ltd., Ibaraki, Japan) according to the manufacturer's instructions, and the serum titer of HCV was determined by real-time quantitative PCR using TaqMan EZ RT-PCR Core Reagent and an ABI Prism 7500 sequence detector system as described previously (Takeuchi et al., 1999).

RNA Isolation and TaqMan Gene Expression Assays. Body weight was measured, and the liver was harvested from each mouse at 17 to 19 weeks of age. Total RNA was isolated from liver specimens using TRIzol (Invitrogen, Carlsbad, CA) according to the manufacturer's instructions and then treated with DNase I to remove contaminating genomic DNA. For cDNA synthesis, 80 ng of RNA was reverse-transcribed using a Transcriptor First Strand cDNA Synthesis Kit (Roche Applied Science, Indianapolis, IN) with random hexamer as the primer. The mRNA expression of human ABC transporters, SLC transporters, cytochrome P450 enzymes, and interferon-stimulated genes (ISGs) was quantified by TaqMan Gene Expression Assays on an ABI Prism 7900 system (Applied Biosystems, Foster City, CA) using LightCycler 480 Probe Master (Roche Applied Science) with primers and FAM-TAMRA or FAM-Iowa Black dual-labeled probes (Integrated DNA Technologies, Inc., Coralville, IA) that are specific for human genes. The protocol for PCR was as follows: 50°C for 2 min, 95°C for 10 min, and 40 cycles of 95°C for 15 s and 60°C for 1 min. The assay identification number or sequences of primers and probes used in the present study are listed in Table 1. The specificities of primers and probes to human genes were confirmed by comparing the amplification from human or mouse liver cDNA. No specific amplification was observed when mouse liver cDNA was used as a PCR template for all genes tested (data not shown). HCV RNA content in the livers of PXB mice was also quantified by TaqMan Gene Expression Assays using a cocktail of three forward primers, one reverse primer, and two TaqMan probes (Table 1) as described previously (Cook et al., 2004). The mRNA expression of each gene was quantified using the comparative C_t method, and normalized by the mRNA expression of hGAPDH.

Preparation of Liver Microsomes and Determination of Activities of Cytochrome P450 Enzymes. The microsomal fractions were isolated from the livers of noninfected and HCV-infected PXB mice at 18 or 20 weeks of age as described previously and stored at −70°C until further use (Sugihara et al., 2001). The activities of various P450s were determined in liver microsomes of PXB mice using selective substrates for the human P450 isoforms at appropriate concentrations (Table 2). In brief, 0.2 mg/ml microsomes were preincubated with substrate in 50 mM potassium phosphate buffer (pH 7.4) containing 5 mM $MgCl_2$ at 37°C for 5 min, and, subsequently, 2 mM NADPH was added to start the enzyme reaction. After the incubation at 37°C for 30 min (CYP1A2, CYP2C9, and CYP2C19), 15 min (CYP2D6), or 10 min (CYP3A4), the reaction was terminated by the addition of 150 μl of acetonitrile containing 7-hydroxycoumarin as an internal standard to 100 μl of incubation mixture. Samples were then centrifuged at 3000 rpm for 10 min at 4°C to precipitate the protein, and 10 μl of supernatant was analyzed by liquid chromatography (LC)-tandem mass spectrometry (MS/MS) to quantify the formation of metabolite. For the detection of acetaminophen, the supernatant as well as standard curves were further diluted with 5 mM ammonium acetate to ensure that the signal of each analyte was within the linear range of LC-MS/MS analysis. All of the experiments were conducted in triplicate.

LC-MS/MS Analysis. LC-MS/MS was performed on a Shimadzu high-performance liquid chromatography system with two LC-10ADvp pumps and the SCL-10Avp controller (Shimadzu Scientific Instruments, Columbia, MD) and an ABI Sciex API 4000 (Applied Biosystems). Samples were separated on a Hypersil BDS C18 column (50 × 2.1 mm, 5 μm; Thermo Fisher Scientific, Waltham, MA) with mobile phase A (0.1% formic acid in 5 mM ammonium acetate) and B (0.1% formic acid in acetonitrile/methanol 50/50, v/v) at a flow rate of 0.4 ml/min. High-performance liquid chromatography gradient programs were as follows: for CYP1A2, CYP2C9, and CYP2C19 assays,

TABLE 1

Assay identification number or sequences of primers and probes used for the TaqMan gene expression assays

Gene Name	RefSeq Identification	Assay Identification	Sequences (5′ to 3′)		
			Forward Primer	Reverse Primer	Probe
ABC transporters					
P-gp	NM_000927	Hs01067802_m1			
MDR3	NM_000443		CATCAATGACACCACTGAACTCAA	AACCTTGTCACCAATTCCTTCAC	CGCGGCTAACAGATGACATCTCCAAAA
BSEP	NM_003742		GGGCCATTGTACGAGATCCTAA	TGCACCGTCTTTTCACTTTCTG	TCTTGCTACTAGATGAAGCCACTTCTGCCTTAGA
MRP1	NM_004996		CATCGTGCAGGCGAGTGT	TCCTCACGGTGATGCTGTTC	TGACAGCATCGAGCGACGGCC
MRP2	NM_000392	Hs00166123_m1			
MRP3	NM_003786	Hs00358656_m1			
MRP4	NM_005845	Hs00195260_m1			
BCRP	NM_004827		CAGGTCTGTTGGTCAATCTCACA	TCCATATCGTGGAATGCTGAAG	CCATTGCATCTTGGCTGTCATGGCTT
SLC transporters					
NTCP	NM_003049		CCATGACACCACTCTTGATTGC	CGTCTGCACCGTCCATTG	ACCTCCTCCCTGATGCCTTTTATTGGC
OCT1	NM_003057	Hs00427550_m1			
OAT2	NM_006672		CTGCTAGTGTCCTCCGATATGAAG	GCACCGTAGGGTACAACTCTGAA	AAGCTGCCTTCACCACTGCCTACCTG
OATP1B1	NM_006446		GTACCACTTTCTTATTGCAACTCAGACT	CAGGGTGAGATGTAAGTTATTCCATTG	TCCACAGACTGGTTCCCATTGACTTTCA
OATP1B3	NM_019844	Hs00251986_m1			
OATP2B1	NM_007256		TCCTGTTTGCAGTGACCATGA	CACCTTCTGGCATCTGGTTAATG	CAGCCTCATGCTGCGCCTTTATGTG
Cytochrome P450 enzymes					
CYP1A1	NM_000499		TGGTCAAGGAGCACTACAAAACC	AGGTCCAAGACGATGTTAATGATCT	ATGAGAACGCCAATGTCCAGCTGTCA
CYP1A2	NM_000761		GGAGACCTTCCGACACTCCTC	CGTTGTGTCCCTTGTTGTGC	TTCTTGCCCTTCACCATCCCCAC
CYP2A6	NM_000762	Hs00711162_s1			
CYP2B6	NM_000767		TTGTTCTACCAGACTTTTTCACTCATC	GGAAAGTATTTCAAGAAGCCAGAGA	TCTGTATTCGGCCAGCTGTTTGAGCTC
CYP2C8	NM_000770	Hs00426387_m1			
CYP2C9	NM_000771	Hs00426397_m1			
CYP2C18	NM_000772	Hs00426403_m1			
CYP2C19	NM_000769	Hs00426380_m1			
CYP2D6	NM_000106	Hs00164385_m1			
CYP2E1	NM_000773	Hs00559368_m1			
CYP3A4	NM_017460		CAGGAGGAAATTGATGCAGTTTT	GTCAAGATACTCCATCTGTAGCACAGT	CCCAATAAGGCACCACCCACCTATGA
CYP3A5	NM_000777		TGGACTTTTTAAGAGACTGGGAATTC	AAATTTCCAGAGACCCTGACGAT	CACACCTCTGCCTTTGTTGGGAAATGTT
ISGs					
CIG5	NM_080657		AGATGTTTCTGAAGCGAGGA	GCAGACAATGGCAGTTACTC	TGGATTGGTAGAGCGGAAAGTGGA
G1P2	NM_005101		CTCATCTTTGCCAGTACAGG	AGCTCTGACACCGACAT	CCATGGGCTGGGACCTGACG
G1P3	NM_002038		AAGGCCCTGACCTTCAT	ATTCAGGATCGCAGACCA	AGGAGGACTCGCAGTCGCC
HSXIAPAF1	NM_017523		CTTGAGCACCAGCAGG	GCATGTCCAGTTTGCAGA	TCATAAGGCCAATGAGTGCCAGGA
IFI27	NM_005532		GTAGTTTTGCCCCTGGC	GACATCATCTTGGCTGCT	TGTGATTGGAGGAGTTGTGGCTGT
IFI35	NM_005533		CAAGATGAGGCTGTGGGA	AGACTTAGGCACTTCCGG	CCCCAAAGACAAGGTCCCATTTTCAG
IFI44	NM_006417		GCTACCCTCAGCTCTAGC	CGCTTCCCTCCAAAATGA	ACTGCCATACTTCTTGATCTGTTGTACTGT
IFIT2	NM_001547		AGGAAGATTTCTGAAGAGTGC	GTTCCAGGTGAAATGGCA	CACTGCAACCATGAGTGAGAACAATAAGAA
IFITM1	NM_003641		TCCTCATGACCATTGGATTCATC	CCGTTTTTCCTGTATTATCTGTAACATAA	AGACTGTCACAGAGCCGAATACCA
IRF7	NM_001572		GCAGCGTGAGGGTGTGTCTT	GGAAGCACTCGATGTCGTCAT	CCTGTCCAGCGCCAACAGCC
IRF9/ISGF3G	NM_006084	Hs00196051_m1			
MX1	NM_002462		AAGGAATGGGAATCAGTCATGAG	TCTATTAGAGTCAGATCCGGGACAT	CACCCTGGAGATCAGCTCCCGA
MX2	NM_002463		CTAGAGCTTCAGGACCCT	TGATGGTCAGGTCTGGAAC	CGTTCTGGGCTTTGTGTATCTCTTTCTC
OAS1	NM_016816		TGTGTGTCCAAGGTGGTAAAGG	CAACCAGGTCAGCGTCAGATC	CCTCAGGCAAGGGCACCACCCT
OAS2	NM_016817	Hs00942643_m1			
OAS3	NM_006187	Hs00196324_m1			
OASL	NM_003733	Hs00984390_m1			
SP110	NM_004510		CAAAGCGATGAGATCCTGAG	CTGAGTCTTCTTCCGCATTC	CTTGTCATTGGTCACTGAAGTGCTTCT
STAT1	NM_007315		GTGGAAAGACAGCCCTGCAT	ACTGGACCCCTGTCTTCAAGAC	AACGCACCCTCAGAGGCCGC
TLR3	NM_003265	Hs01551078_m1			
TNFSF10	NM_003810		TGCGTGCTGATCGTGATCTT	GTACTTGTCCTGCATCTGCTTCA	TGCTCCTGCAGTCTCTCTGTGTGGCT
TRIM22	NM_006074		GCAGGAGTTTGTGACCAA	AGAGGTTCTGTCAGGAGC	CCAAGGGAGCAGTGCAATGGATTT

DRUG METABOLISM AND DISPOSITION DMD

TABLE 1—*Continued.*

Gene Name	RefSeq Identification	Assay Identification	Sequences (5′ to 3′)		
			Forward Primer	Reverse Primer	Probe
Others					
GAPDH	NM_002046		GAAGGTGAAGGTCGGAGTC	GAAGATGGTGATGGGATTTC	CAAGCTTCCCGTTCTCAGCC
HCV (5′-UTR)			GCGACACTCCACCATAGATCACT	CACTCGCAAGCACCCTATCA	AGGCCTTTCGCGACCCAACACTACTC
			CGACACTCCACCATGAATCACT		AGGCCTTTCGCAACCCAACGCTACT
			CACTCCGCCATGAAYCACT[a]		

UTR, untranslated region.
[a] Y = C or T.

1) mobile phase B was maintained at 5% for 1.0 min, 2) increased linearly to 90% from 1.0 to 2.0 min and maintained to 3.0 min, and 3) brought back to the initial concentration linearly from 3.0 to 3.1 min for reequilibration, total run time 4.0 min; for CYP2D6 assay, 1) mobile phase B was maintained at 5% for 1.0 min, 2) increased linearly to 95% from 1.0 to 2.0 min and maintained to 4.0 min, and 3) brought back to the initial concentration linearly from 4.0 to 4.1 min for reequilibration, total run time 6.0 min; and for CYP3A4 assay, 1) mobile phase B was maintained at 5% for 1.0 min, 2) increased linearly to 95% from 1.0 to 2.0 min and maintained to 3.0 min, and 3) brought back to the initial concentration linearly from 3.0 to 3.1 min for reequilibration, total run time 4.0 min. The MS/MS parameters and linear range of standard curves (limit of detection to maximum concentration) are listed for each metabolite in Table 2. Data were collected and processed using Sciex Analyst 1.4.2 data collection and integration software.

Statistical Analysis. Statistical analysis was performed by Student's *t* test using GraphPad Prism (version 4). Asterisks represent significant differences (*, $P < 0.05$, **, $P < 0.01$, and ***, $P < 0.001$, respectively) between noninfected and HCV-infected PXB mice.

Results

Human Albumin Concentration and HCV Titers in PXB Mice. Sex, human albumin concentration in the blood, body weight, serum HCV titers, and HCV RNA content in the liver are summarized in Table 3 for each mouse. The sex of PXB mice did not affect the activity of human cytochrome P450 enzymes derived from the human hepatocytes inside the host mouse liver (supplemental data). The average concentration of human albumin in the blood was not significantly different between noninfected and HCV-infected PXB mice. Accordingly, the replacement index of human hepatocytes estimated from the albumin concentration was similar between the two groups. Although body weight at the time of liver isolation was significantly higher in HCV-infected PXB mice than in noninfected mice for those used for the preparation of total liver RNA, the difference was not statistically significant in those used for the preparation of liver microsomes. Indeed, unpublished observations (C. Tateno) with different batches of HCV-infected mice suggested that HCV infection does not significantly affect the body weight of either male or female PXB mice. Serum HCV titers were determined in HCV-infected PXB mice, and HCV RNA content in the liver was measured in both noninfected and HCV-infected groups. A significant amount of HCV RNA was detected in both the serum and liver of HCV-infected mice, whereas HCV RNA was not detected in the liver of noninfected mice. These results confirmed that PXB mice were successfully infected by HCV.

Activation of Interferon-Signaling Pathways in HCV-Infected PXB Mice. Previous reports suggested that chronic infection with HCV is accompanied by the up-regulation of genes related to the interferon-signaling pathways in human patients (Smith et al., 2006). To corroborate the relevance of our experimental model in PXB mice to clinical HCV infection, the mRNA expression of human ISGs observed to be activated in HCV-infected patients was quantified in the livers of noninfected and HCV-infected mice. Fourteen of 22 ISGs investigated exhibited a significant increase in mRNA expression in the livers of HCV-infected PXB mice compared with that in noninfected mice (Fig. 1). The mRNA expression of MX2 was below the limit of detection in both groups. These results suggest that the interferon signaling pathways are activated by HCV infection in PXB mice, which is similar to what is observed in patients with chronic HCV infection.

mRNA Expression of Human ABC and SLC Transporters. The mRNA expression of major human hepatic ABC and SLC transporters was quantified in the livers of noninfected and HCV-infected PXB mice (Fig. 2). A significant increase in mRNA expression was ob-

DMD DRUG METABOLISM AND DISPOSITION aspet

TABLE 2

Substrate concentration and analytical parameters for each metabolite in MS/MS

Enzyme	Substrate	Metabolite	Mass Transition (*m/z*)	Mode	CE	DP	Linear Range
					eV	*eV*	
CYP1A2	Phenacetin (10 μM)	Acetaminophen	152.13 > 110.15	ESI+	22	46	10 nM–10 μM
CYP2C9	Diclofenac (5 μM)	4′-Hydroxydiclofenac	312.09 > 230.01	ESI+	45	41	1 nM–1 μM
CYP2C19	(*S*)-Mephenytoin (50 μM)	4′-Hydroxymephenytoin	235.10 > 150.21	ESI+	24	56	1 nM–1 μM
CYP2D6	Dextromethorphan (5 μM)	Dextrorphan	258.17 > 157.10	ESI+	51	81	1 nM–1 μM
CYP3A4	Midazolam (1 μM)	1′-Hydroxymidazolam	341.82 > 203.20	ESI+	38	71	1 nM–1 μM

CE, collision energy; DP, declustering potential; ESI, electrospray ionization.

TABLE 3

Human albumin concentration, estimated replacement index, body weight, and HCV content in the serum and liver of PXB mice

Animal	Sex	h-Alb	Estimated RI	Body Weight	Serum HCV Titer (10^7 copies/ml)	HCV RNA Content in the Liver (Relative to hGAPDH)
		mg/ml	%	*g*		
PXB mice used for the preparation of total liver RNA						
Noninfected						
PXB41-18	Male	6.3	74.2	14.4	—[a]	N.D.
PXB41-25	Male	8.2	82.3	13.7	—	N.D.
PXB42-1	Male	12.2	94.6	15.0	—	N.D.
Mean ± S.D.		8.9 ± 3.0	83.7 ± 10.3	14.3 ± 0.6	—	—
HCV-infected						
PXB36-11	Male	5.3	68.9	17.2	5.15	4.95×10^{-3}
PXB36-23	Male	7.7	80.4	16.8	5.52	3.53×10^{-3}
PXB38-11	Male	5.8	71.7	16.2	2.12	3.16×10^{-3}
Mean ± S.D.		6.3 ± 1.3	73.7 ± 6.0	16.7 ± 0.5*	4.26 ± 1.87	$3.88 \times 10^{-3} \pm 9.46 \times 10^{-4}$
PXB mice used for the preparation of liver microsomes						
Noninfected						
PXB22-47	Female	6.3	74.2	19.8	—	—
PXB22-48	Female	7.3	78.7	11.5	—	—
PXB22-57	Female	5.2	68.2	14.7	—	—
Mean ± S.D.		6.3 ± 1.1	73.7 ± 5.3	15.3 ± 4.2	—	—
HCV-infected						
PXB86-13	Male	6.3	74.2	22.8	6.56	—
PXB86-26	Female	3.5	55.9	19.4	0.806	—
PXB86-33	Male	6.4	74.6	22.1	4.66	—
Mean ± S.D.		5.4 ± 1.6	68.2 ± 10.7	21.4 ± 1.8	4.01 ± 2.93	—

h-Alb, human albumin; RI, replacement index; N.D., not detected.
* $P < 0.01$, significantly different between noninfected and HCV-infected PXB mice.
[a] —, not determined.

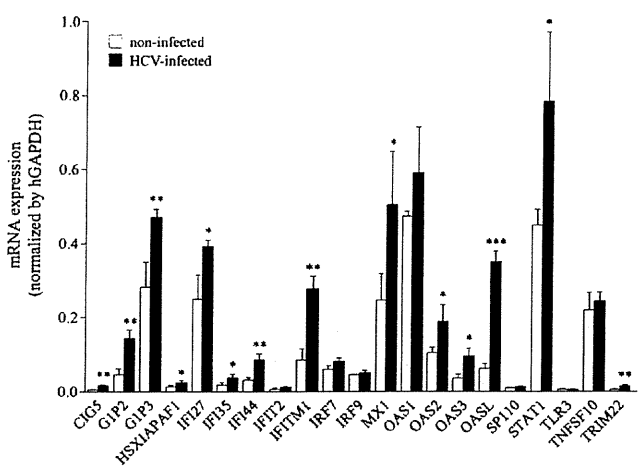

FIG. 1. Activation of interferon signaling pathways in HCV-infected PXB mice. The mRNA expression of human interferon-stimulated genes was measured in the livers of noninfected and HCV-infected PXB mice by TaqMan Gene Expression Assays as described under *Materials and Methods*, and the data were normalized by the mRNA expression of hGAPDH. Results are presented as the mean ± S.D. of three mice. □, mRNA expression in noninfected PXB mice; ■, mRNA expression in HCV-infected PXB mice. *, $P < 0.05$; **, $P < 0.01$; ***, $P < 0.001$, significantly different between noninfected and HCV-infected mice.

served for MRP4 and OATP2B1 in HCV-infected PXB mice compared with that in noninfected mice. In contrast, OCT1 was significantly decreased in HCV-infected PXB mice compared with that in their noninfected controls. The mRNA expression of MRP1 was below the limit of detection in both noninfected and HCV-infected groups. The mRNA levels of other ABC and SLC transporters, including P-gp, MDR3, BSEP, MRP2, MRP3, NTCP, OAT2, OATP1B1, and OATP1B3, were comparable between the two groups.

mRNA Expression of Human Cytochrome P450 Enzymes. The mRNA expression of 12 human cytochrome P450 genes, *CYP1A1*, *CYP1A2*, *CYP2A6*, *CYP2B6*, *CYP2C8*, *CYP2C9*, *CYP2C18*, *CYP2C19*, *CYP2D6*, *CYP2E1*, *CYP3A4*, and *CYP3A5*, was investigated in the livers of noninfected and HCV-infected PXB mice (Fig. 3). The mRNA expression of these genes was not statistically different between the two groups with the exception of significantly lower expression of CYP2D6 in HCV-infected mice.

Activity of Human Cytochrome P450 Enzymes. The activities of five major human cytochrome P450 enzymes, namely, CYP1A2, CYP2C9, CYP2C19, CYP2D6, and CYP3A4, were investigated in the liver microsomes of noninfected and HCV-infected PXB mice (Fig. 4). The metabolic activity in the liver microsomes from uPA/SCID mice for each probe substrate was comparable to or lower than that in human liver microsomes (C. Tateno, unpublished observations). Taking into account the fact that the livers of PXB mice are nearly completely (>70%) replaced with human hepatocytes, the background activity from remaining mouse hepatocyte in PXB

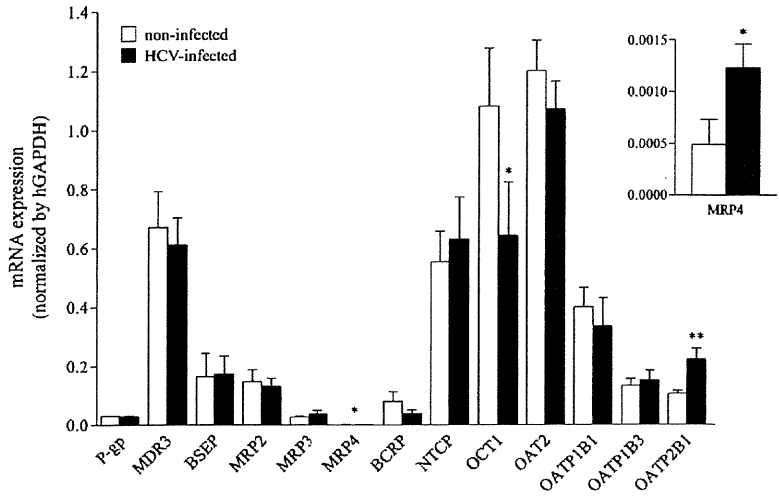

FIG. 2. mRNA expression profiles of drug transporters in PXB mice. The mRNA expression of human ABC and SLC transporters was measured in the livers of noninfected (□) and HCV-infected (■) PXB mice by TaqMan Gene Expression Assays, and the data are presented as described in the legend to Fig. 1. The inset represents the magnification of the mRNA expression of MRP4.

mice is minor. The metabolic activity of CYP1A2 was significantly lower in HCV-infected PXB mice than in noninfected PXB mice. The activities of other P450s were similar between noninfected and HCV-infected PXB mice.

Discussion

In the present study, the effect of HCV infection on the mRNA expression profiles of human ABC and SLC transporters and cytochrome P450 enzymes in PXB mice was investigated. The primers and probes specific for human genes were used in the TaqMan gene expression assays to exclude the background amplification of homologous genes from the host mouse liver. In addition, we have characterized enzymatic activities of major human P450s in the microsomes isolated from the livers of PXB mice.

The body weight and human albumin concentration in the blood of PXB mice were similar between noninfected and HCV-infected groups, suggesting that the inoculation of HCV does not affect the growth of transplanted human hepatocytes inside the host mouse liver or maturation of the mice (Table 3). A profound effect of HCV infection was observed on the status of interferon-signaling pathways, for which mRNA expression of a series of ISGs was significantly higher in the livers of HCV-infected PXB mice compared with that of noninfected controls (Fig. 1). The up-regulation of ISGs are in good agreement with the observation in patients with chronic HCV infection and chimpanzees with acute HCV infection (Su et al., 2002; Smith et al., 2006). In addition, these data are similar to the results published previously by Walters et al. (2006) who also used the human hepatocyte chimeric mouse model to examine the regulation of overall hepatic gene expression by HCV genotype 1a infection with microarray technology. It is of note that the effect of HCV infection on the expression of ISGs was comparable between genotype 1a (Walters et al., 2006) and 1b (this study). It is likely that there is no marked difference between the two HCV genotypes in terms of their effects on gene expression. It has been previously demonstrated that viremia in PXB mice can be reduced by treatment with IFN-α or pegylated-IFN as in human patients (Umehara et al., 2006; Hiraga et al., 2007; Inoue et al., 2007). The presence of functional interferon signaling pathways in PXB mice, suggested by the up-regulation of a number of ISGs by HCV infection, provides a rationale for the efficacy of those antiviral agents in this model. These observations warrant the use of PXB mice as an in vivo model for the primary infection of the liver by HCV to investigate the effects of novel anti-HCV compounds on suppressing the replication of HCV.

There were, in general, few marked differences in the mRNA expression of human ABC and SLC transporters and cytochrome P450 enzymes in the liver between noninfected and HCV-infected PXB mice with some exceptions, e.g., significantly higher expression

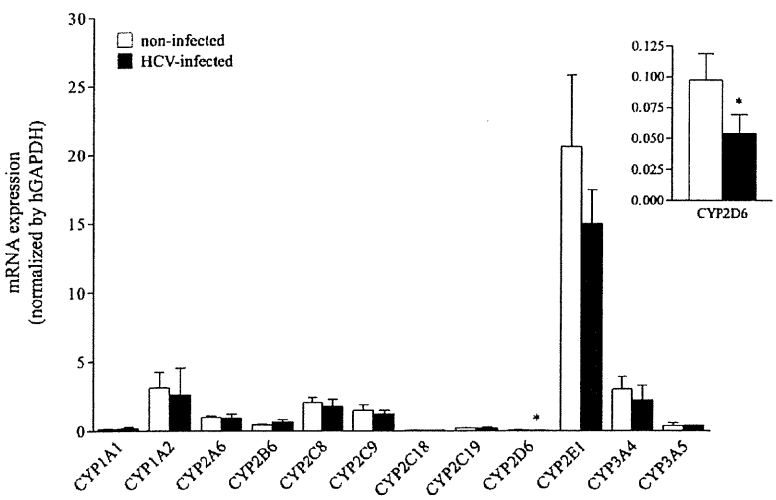

FIG. 3. mRNA expression profiles of drug-metabolizing enzymes in PXB mice. The mRNA expression of human cytochrome P450 enzymes was measured in the livers of noninfected (□) and HCV-infected (■) PXB mice by TaqMan Gene Expression Assays, and the data are presented as described in the legend to Fig. 1. The inset represents the magnification of the mRNA expression of CYP2D6.

DRUG METABOLISM AND DISPOSITION DMD aspet

DRUG METABOLISM AND DISPOSITION DMD

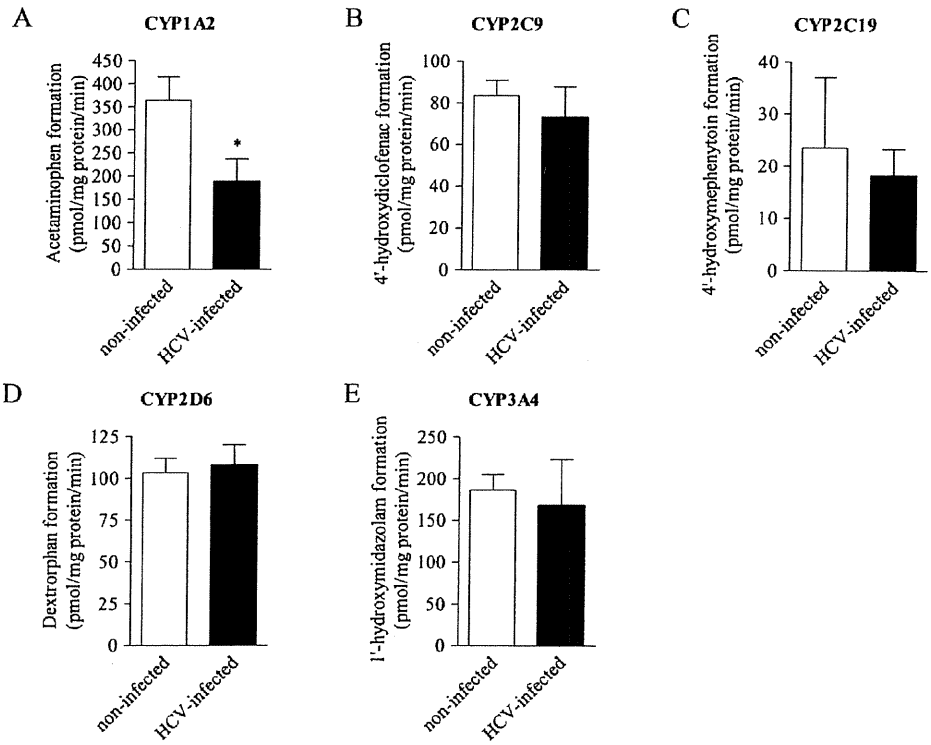

FIG. 4. Activity of human cytochrome P450 enzymes in PXB mice. The activities of five major human cytochrome P450 enzymes, i.e., CYP1A2 (A), CYP2C9 (B), CYP2C19 (C), CYP2D6 (D), and CYP3A4 (E), were measured in the liver microsomes of noninfected and HCV-infected PXB mice as described under *Materials and Methods*. Results are presented as the mean ± S.D. of three mice. □, metabolic activity in noninfected PXB mice; ■, metabolic activity in HCV-infected PXB mice. *, $P < 0.05$, significantly different between noninfected and HCV-infected mice.

of MRP4 and OATP2B1 and lower expression of OCT1 and CYP2D6 in HCV-infected mice than in noninfected mice (Figs. 2 and 3). Likewise, the activities of major human cytochrome P450 enzymes were similar between noninfected and HCV-infected PXB mice except for CYP1A2, which exhibited a significantly lower activity in HCV-infected PXB mice than in noninfected mice (Fig. 4). The effect of HCV infection on the mRNA expression and enzymatic activity of CYP1A2 and CYP2D6 was not consistent. The change in mRNA expression of CYP2D6 might not be sufficient to affect its enzymatic activity, whereas posttranscriptional effects of HCV infection may explain the decreased enzymatic activity of CYP1A2 regardless of unchanged mRNA expression. In consideration of the induction of many ISGs at the mRNA level, it is likely that the effect of HCV infection on the expression of pharmacokinetics-related genes would also be observed, if any, at the transcriptional level (CYP1A2 might be an exception). HCV infection probably affects gene expression via direct interference by virus infection, that is, the innate antiviral response and/or indirect interference by adaptive HCV-specific immune response, oxidative stress, and liver disease associated with chronic infection (Pawlotsky, 1998; Missale et al., 2004). PXB mice are immunocompromised because of their genetic background and thus lack the adaptive immune response and liver disease associated with HCV infection: i.e., there was no hepatocyte damage or inflammation in the liver of infected chimeric mice (Hiraga et al., 2007). HCV infection will thus affect gene expression only through the innate antiviral response in our experimental model. The similar expression profiles of drug transporters and metabolizing enzymes between noninfected and HCV-infected PXB mice suggest that innate antiviral signaling pathways play only a minor role in the regulation of mRNA expression of these genes.

There have been several reports regarding the aberrant mRNA expression of drug transporters and metabolizing enzymes in patients with HCV infection compared with those without infection or healthy volunteers. Hinoshita et al. (2001) have demonstrated that the mRNA expression of P-gp, MDR3, MRP1, MRP2, and MRP3 in the noncancerous region in the liver of patients with hepatic tumor tends to be lower in HCV-infected groups than in noninfected ones. On the other hand, Ros et al. (2003) have reported increased mRNA expression of P-gp and MRP3 in the livers of patients with HCV infection compared with healthy volunteers, whereas there was no significant difference for MRP2. Nakai et al. (2001) have performed a comprehensive study of variation in the mRNA levels of drug transporters and metabolizing enzymes in patients with chronic hepatitis C using quantitative real-time PCR and observed clear correlations between fibrosis stage and mRNA levels of CYP1A2, CYP2E1, CYP3A4, NTCP, OCT1, and OATP1B1 in the liver, whereas no fibrosis stage-dependent differences were observed for other transporters and enzymes that included P-gp, MDR3, MRP1, MRP2, and MRP3 (Nakai et al., 2008). Intriguingly, these clinical observations are inconsistent with the present findings in PXB mice in which HCV infection affects gene expression primarily through the innate antiviral response. The altered expression of drug transporters and metabolizing enzymes in clinical patients might be ascribed to the indirect interference by HCV infection or secondary effects as a result of the development of liver fibrosis or other hepatic dysfunction resulting from HCV infection. Indeed, serum levels or spontaneous productions by peripheral blood mononuclear cells of inflammatory cytokines such as tumor necrosis factor-α, interleukin-1β, and interleukin-6 were elevated in HCV-infected patients compared with those in healthy subjects (Kishihara et al., 1996; Huang et al., 1999; Cotler et al., 2001). In addition, several lines of evidence suggest perturbation of the expression of drug transporters and metabolizing enzymes by these cytokines both in vivo and in vitro (Lee and Piquette-Miller, 2003; Geier et al., 2005; Renton, 2005; Vee et al., 2009). Oxidative stress and liver diseases including cirrhosis and hepatocellular carcinoma, which are prevalent in patients with chronic HCV infection, also compromise the physiological expression of drug transporters (Bonin et al., 2002; Toyoda et al., 2008). This complex nature of HCV infection and progression to liver disease may

DRUG METABOLISM AND DISPOSITION DMD aspet

account for the controversial findings regarding the expression of pharmacokinetics-related genes in clinical patients with HCV infection, although the possibility of a difference in the patient population cannot be ruled out.

Because all PXB mice used in the present study are derived from a single donor hepatocyte, future studies are necessary to generalize the present findings by characterizing different batches of PXB mice originated from other donor hepatocytes. Nevertheless, the present study has clearly demonstrated that the infection of PXB mice, the chimeric mice with humanized liver, by HCV triggers the activation of interferon-signaling pathways as observed in human patients with chronic infection, but in general does not have a significant impact on the mRNA expression profiles of human ABC and SLC transporters or on the mRNA expression and enzymatic activity of cytochrome P450 enzymes. These results suggest that the pharmacokinetic behavior of small molecule antiviral therapies such as protease and polymerase inhibitors is likely to be comparable between HCV-infected and noninfected PXB mice. The PXB mouse model is a good model to study the effects of novel anti-HCV compounds in the primary treatment of HCV infection on suppressing the replication of HCV and therefore to investigate the relationship of the pharmacokinetics and pharmacodynamics of such therapies. However, caution is needed in the translation of this relationship to HCV-infected patients because PXB mice are immunocompromised based on their genetic background (SCID), and thus this mouse model does not accurately reflect the liver disease and immune response such as the increase in the levels of inflammatory cytokines observed in patients with chronic HCV infection, which may lead to changes in drug transporter and metabolizing enzyme expression.

Acknowledgments. We thank Drs. Yasuhisa Adachi and Shin-ichi Ninomiya for their technical assistance in the microsome assays.

References

Bartenschlager R (2005) The hepatitis C virus replicon system: from basic research to clinical application. *J Hepatol* **43**:210–216.

Bonin S, Pascolo L, Crocé LS, Stanta G, and Tiribelli C (2002) Gene expression of ABC proteins in hepatocellular carcinoma, perineoplastic tissue, and liver diseases. *Mol Med* **8**:318–325.

Buck M (2008) Direct infection and replication of naturally occurring hepatitis C virus genotypes 1, 2, 3 and 4 in normal human hepatocyte cultures. *PLoS One* **3**:e2660.

Chandra P and Brouwer KL (2004) The complexities of hepatic drug transport: current knowledge and emerging concepts. *Pharm Res* **21**:719–735.

Cook L, Ng KW, Bagabag A, Corey L, and Jerome KR (2004) Use of the MagNA pure LC automated nucleic acid extraction system followed by real-time reverse transcription-PCR for ultrasensitive quantitation of hepatitis C virus RNA. *J Clin Microbiol* **42**:4130–4136.

Coller SJ, Reddy KR, McCone J, Wolfe DL, Liu A, Craft TR, Ferris MW, Conrad AJ, Albrecht J, Morrissey M, Ganger DR, Rosenblate H, Blatt LM, Jensen DM, and Taylor MW (2001) An analysis of acute changes in interleukin-6 levels after treatment of hepatitis C with consensus interferon. *J Interferon Cytokine Res* **21**:1011–1019.

Dobson PD and Kell DB (2008) Carrier-mediated cellular uptake of pharmaceutical drugs: an exception or the rule? *Nat Rev Drug Discov* **7**:205–220.

Geier A, Dietrich CG, Voigt S, Ananthanarayanan M, Lammert F, Schmitz A, Trauner M, Wasmuth HE, Boraschi D, Balasubramaniyan N, Suchy FJ, Matern S, and Gartung C (2005) Cytokine-dependent regulation of hepatic organic anion transporter gene transactivators in mouse liver. *Am J Physiol Gastrointest Liver Physiol* **289**:G831–G841.

Gonzalez FJ (1990) Molecular genetics of the P-450 superfamily. *Pharmacol Ther* **45**:1–38.

Hinoshita E, Taguchi K, Inokuchi A, Uchiumi T, Kinukawa N, Shimada M, Tsuneyoshi M, Sugimachi K, and Kuwano M (2001) Decreased expression of an ATP-binding cassette transporter, MRP2, in human livers with hepatitis C virus infection. *J Hepatol* **35**:765–773.

Hiraga N, Imamura M, Tsuge M, Noguchi C, Takahashi S, Iwao E, Fujimoto Y, Abe H, Maekawa T, Ochi H, Tateno C, Yoshizato K, Sakai A, Sakai Y, Honda M, Kaneko S, Wakita T, and Chayama K (2007) Infection of human hepatocyte chimeric mouse with genetically engineered hepatitis C virus and its susceptibility to interferon. *FEBS Lett* **581**:1983–1987.

Huang YS, Hwang SJ, Chan CY, Wu JC, Chao Y, Chang FY, and Lee SD (1999) Serum levels of cytokines in hepatitis C-related liver disease: a longitudinal study. *Zhonghua Yi Xue Za Zhi (Taipei)* **62**:327–333.

Inoue K, Umehara T, Ruegg UT, Yasui F, Watanabe T, Yasuda H, Dumont JM, Scalfaro P, Yoshiba M, and Kohara M (2007) Evaluation of a cyclophilin inhibitor in hepatitis C virus-infected chimeric mice in vivo. *Hepatology* **45**:921–928.

Kishihara Y, Hayashi J, Yoshimura E, Yamaji K, Nakashima K, and Kashiwagi S (1996) IL-1β and TNF-α produced by peripheral blood mononuclear cells before and during interferon therapy in patients with chronic hepatitis C. *Dig Dis Sci* **41**:315–321.

Kremsdorf D and Brezillon N (2007) New animal models for hepatitis C viral infection and pathogenesis studies. *World J Gastroenterol* **13**:2427–2435.

Lanford RE, Bigger C, Bassett S, and Klimpel G (2001) The chimpanzee model of hepatitis C virus infections. *ILAR J* **42**:117–126.

Lee G and Piquette-Miller M (2003) Cytokines alter the expression and activity of the multidrug resistance transporters in human hepatoma cell lines; analysis using RT-PCR and cDNA microarrays. *J Pharm Sci* **92**:2152–2163.

Littlejohn M, Locarnini S, and Bartholomeusz A (1998) Targets for inhibition of hepatitis C virus replication. *Antivir Ther* **3**:83–91.

Meyer UA (1996) Overview of enzymes of drug metabolism. *J Pharmacokinet Biopharm* **24**:449–459.

Missale G, Cariani E, and Ferrari C (2004) Role of viral and host factors in HCV persistence: which lesson for therapeutic and preventive strategies? *Dig Liver Dis* **36**:703–711.

Nakai K, Tanaka H, Hanada K, Ogata H, Suzuki F, Kumada H, Miyajima A, Ishida S, Sunouchi M, Habano W, Kamikawa Y, Kubota K, Kita J, Ozawa S, and Ohno Y (2008) Decreased expression of cytochromes P450 1A2, 2E1, and 3A4 and drug transporters Na^+-taurocholate-cotransporting polypeptide, organic cation transporter 1, and organic anion-transporting peptide-C correlates with the progression of liver fibrosis in chronic hepatitis C patients. *Drug Metab Dispos* **36**:1786–1793.

Nishimura M, Yoshitsugu H, Yokoi T, Tateno C, Kataoka M, Horie T, Yoshizato K, and Naito S (2005) Evaluation of mRNA expression of human drug-metabolizing enzymes and transporters in chimeric mouse with humanized liver. *Xenobiotica* **35**:877–890.

Pawlotsky JM (1998) Hepatitis C virus infection: virus/host interactions. *J Viral Hepat* **5(Suppl 1)**:3–8.

Rendic S and Di Carlo FJ (1997) Human cytochrome P450 enzymes: a status report summarizing their reactions, substrates, inducers, and inhibitors. *Drug Metab Rev* **29**:413–580.

Renton KW (2005) Regulation of drug metabolism and disposition during inflammation and infection. *Expert Opin Drug Metab Toxicol* **1**:629–640.

Ros JE, Libbrecht L, Geuken M, Jansen PL, and Roskams TA (2003) High expression of MDR1, MRP1, and MRP3 in the hepatic progenitor cell compartment and hepatocytes in severe human liver disease. *J Pathol* **200**:553–560.

Shitara Y, Horie T, and Sugiyama Y (2006) Transporters as a determinant of drug clearance and tissue distribution. *Eur J Pharm Sci* **27**:425–446.

Smith MW, Walters KA, Korth MJ, Fitzgibbon M, Proll S, Thompson JC, Yeh MM, Shuhart MC, Furlong JC, Cox PP, Thomas DL, Phillips JD, Kushner JP, Fausto N, Carithers RL Jr, and Katze MG (2006) Gene expression patterns that correlate with hepatitis C and early progression to fibrosis in liver transplant recipients. *Gastroenterology* **130**:179–187.

Su AI, Pezacki JP, Wodicka L, Brideau AD, Supekova L, Thimme R, Wieland S, Bukh J, Purcell RH, Schultz PG, and Chisari FV (2002) Genomic analysis of the host response to hepatitis C virus infection. *Proc Natl Acad Sci USA* **99**:15669–15674.

Sugihara K, Kitamura S, Yamada T, Ohta S, Yamashita K, Yasuda M, and Fujii-Kuriyama Y (2001) Aryl hydrocarbon receptor (AhR)-mediated induction of xanthine oxidase/xanthine dehydrogenase activity by 2,3,7,8-tetrachlorodibenzo-*p*-dioxin. *Biochem Biophys Res Commun* **281**:1093–1099.

Takeuchi T, Katsume A, Tanaka T, Abe A, Inoue K, Tsukiyama-Kohara K, Kawaguchi R, Tanaka S, and Kohara M (1999) Real-time detection system for quantification of hepatitis C virus genome. *Gastroenterology* **116**:636–642.

Tateno C, Yoshizane Y, Saito N, Kataoka M, Utoh R, Yamasaki C, Tachibana A, Soeno Y, Asahina K, Hino H, Asahara T, Yokoi T, Furukawa T, and Yoshizato K (2004) Near completely humanized liver in mice shows human-type metabolic responses to drugs. *Am J Pathol* **165**:901–912.

Toyoda Y, Hagiya Y, Adachi T, Hoshijima K, Kuo MT, and Ishikawa T (2008) MRP class of human ATP binding cassette (ABC) transporters: historical background and new research directions. *Xenobiotica* **38**:833–862.

Umehara T, Sudoh M, Yasui F, Matsuda C, Hayashi Y, Chayama K, and Kohara M (2006) Serine palmitoyltransferase inhibitor suppresses HCV replication in a mouse model. *Biochem Biophys Res Commun* **346**:67–73.

Vee ML, Lecureur V, Stieger B, and Fardel O (2009) Regulation of drug transporter expression in human hepatocytes exposed to the proinflammatory cytokines tumor necrosis factor-α or interleukin-6. *Drug Metab Dispos* **37**:685–693.

Wakita T (2007) HCV research and anti-HCV drug discovery: toward the next generation. *Adv Drug Deliv Rev* **59**:1196–1199.

Wakita T (2006) Host-specific response to HCV infection in the chimeric SCID-beige/Alb-uPA mouse model: role of the innate antiviral immune response. *PLoS Pathog* **2**:e59.

Williams JA, Hyland R, Jones BC, Smith DA, Hurst S, Goosen TC, Peterkin V, Koup JR, and Ball SE (2004) Drug-drug interactions for UDP-glucuronosyltransferase substrates: a pharmacokinetic explanation for typically observed low exposure (AUCi/AUC) ratios. *Drug Metab Dispos* **32**:1201–1208.

World Health Organization (1999) Global surveillance and control of hepatitis C. Report of a WHO Consultation organized in collaboration with the Viral Hepatitis Prevention Board, Antwerp, Belgium. *J Viral Hepat* **6**:35–47.

Address correspondence to: Dr. Adrian J. Fretland, Hoffmann-La Roche, 340 Kingsland St., Bldg. 123/1331, Nutley, NJ 07110-1199. E-mail: adrian.fretland@roche.com

Drug Metab. Pharmacokinet. 25 (6): 539–550 (2010).

Regular Article

In Vitro Evaluation of Cytochrome P450 and Glucuronidation Activities in Hepatocytes Isolated from Liver-Humanized Mice

Chihiro YAMASAKI[1,2], Miho KATAOKA[2], Yumiko KATO[1], Masakazu KAKUNI[1], Sadakazu USUDA[3], Yoshihiro OHZONE[4], Sunao MATSUDA[4], Yasuhisa ADACHI[4], Shin-ichi NINOMIYA[4], Toshiyuki ITAMOTO[5], Toshimasa ASAHARA[5], Katsutoshi YOSHIZATO[1,6] and Chise TATENO[1,2,*]

[1]*PhoenixBio, Co., Ltd., Higashihiroshima, Japan*
[2]*Cooperative Link of Unique Science and Technology for Economy Revitalization, Hiroshima Prefectural Institute of Industrial Science and Technology; Higashihiroshima, Japan*
[3]*ImmunoJapan Inc., Tokyo, Japan*
[4]*Sekisui Medical Inc., Tokai, Japan*
[5]*Hiroshima University, Graduate School of Biomedical Sciences, Division of Frontier Medical Science, Department of Surgery and Hiroshima University 21st Century COE Program for Advanced Radiation Casualty Medicine, Programs for Biomedical Research, Hiroshima, Japan*
[6]*Graduate School of Science, Hiroshima University, Higashihiroshima, Japan*

Full text of this paper is available at http://www.jstage.jst.go.jp/browse/dmpk

Summary: Cryopreserved human (h-) hepatocytes are currently regarded as the best *in vitro* model for predicting human intrinsic clearance of xenobiotics. Although fresh h-hepatocytes have greater plating efficiency on dishes and greater metabolic activities than cryopreserved cells, performing reproducible studies using fresh hepatocytes from the same donor and having an "on demand" supply of fresh hepatocytes are not possible. In this study, cryopreserved h-hepatocytes were transplanted into albumin enhancer/promoter-driven, urokinase-type plasminogen activator, transgenic/severe combined immunodeficient (uPA/SCID) mice to produce chimeric mice, the livers of which were largely replaced with h-hepatocytes. We determined whether the chimeric mouse could serve as a novel source of fresh h-hepatocytes for in vitro studies. h-Hepatocytes were isolated from chimeric mice (chimeric hepatocytes), and cytochrome P450 (P450) activities were determined. Compared with cryopreserved cells, the P450 (1A2, 2C9, 2C19, 2D6, 2E1, 3A) activities of fresh chimeric hepatocytes were similar or greater. Moreover, ketoprofen was more actively metabolized through glucuronide conjugates by fresh chimeric hepatocytes than by cryopreserved cells. We conclude that chimeric mice may be a useful tool for supplying fresh h-hepatocytes on demand that provide high and stable phase I enzyme and glucuronidation activities.

Keywords: human hepatocytes; chimeric mice; cytochrome P450; ketoprofen; UDP-glucuronosyltransferase

Introduction

"Chimeric mice" with livers repopulated with human hepatocytes (h-hepatocytes), created using urokinase-type plasminogen activator (uPA)/severe combined immunodeficient (SCID) mice,[1)] were previously established and the expression of both cytochrome P450 enzymes (P450s, CYPs) and phase II enzymes in the liver of these chimeric mice, as well as *in vivo* induction of P450, were examined.[1–4)]

P450 has been found to play an important role in the metabolism of xenobiotics, including drugs. Indeed, approximately 80% of oxidative metabolism is catalyzed by P450s,[5)] and to predict pharmacokinetics and drug interactions precisely, investigation of the pharmacokinetics of a P450 substrate using chimeric mice would be of considerable value.

Species differences are known to exist in the metabolism of ketoprofen.[6)] Ketoprofen is a propionic acid-class nonsteroidal anti-inflammatory drug with analgesic and

Received; May 17, 2010, Accepted; August 12, 2010, J-STAGE Advance Published Date; October 1, 2010
**To whom correspondence should be addressed:* Chise TATENO, Ph.D., *R&D Department, PhoenixBio, Co., Ltd., 3-4-1, Kagamiyama, Higashihiroshima, 739-0046, Japan. Tel/Fax. +81-82-431-0016, E-mail: chise.mukaidani@phoenixbio.co.jp*
This work was supported by CLUSTER and the Regional Science and Technology promotion budget.

antipyretic effects. Rat and mouse P450s primarily metabolize ketoprofen to hydroxyketoprofen.[6,7] In humans, ketoprofen is primarily metabolized by UDP-glucuronosyltransferase (UGT) and is converted to ketoprofen glucuronides.[8] Recently, it was demonstrated that when chimeric mice were administered ketoprofen, glucuronide conjugates were detected in their sera and bile. However, these conjugates are minor products; ketoprofen was primarily hydrolyzed in mice, and the main metabolites were hydrolyzed ketoprofen and glucuronide-conjugated ketoprofen.[7]

The metabolism of chemical entities has been examined using animals in the laboratory, but this approach fails to address differences in drug metabolism that exist between animal species. Because of the species differences in metabolic abilities, fresh h-hepatocytes are a better model for predicting the metabolism of drugs in the human body. For technical reasons, preparing fresh h-hepatocytes ahead of time and performing reproducible studies using the same donor are not possible. Thus, cryopreserved h-hepatocytes have been used, but they are compromised on thawing, resulting in decline and alteration of their normal function. Additionally, h-hepatocytes exhibit large individual differences in P450 activities. The differences might be due to real individual differences and/or the cryopreserving and thawing conditions.

We hypothesized that these practical problems in using h-hepatocytes for in vitro drug testing could be addressed if h-hepatocytes isolated from chimeric mouse livers exhibited human-type drug metabolism capacities in vitro. In the present study, we first determined the yield, viability, and purity of isolated h-hepatocytes from chimeric mice (chimeric hepatocytes). We compared the P450 activities of fresh and cryopreserved chimeric hepatocytes and assessed glucuronide activities toward ketoprofen using fresh and cryopreserved chimeric hepatocytes and cryopreserved donor hepatocytes.

We demonstrate that the chimeric mouse liver is a useful tool that can supply fresh hepatocytes retaining high P450 and UGT activities and allowing reproducible assays using hepatocytes derived from the same donor.

Materials and Methods

Materials: Phenacetin, tolbutamide, *S*-mephenytoin, dextromethorphan, chlorzoxazone, testosterone, ketoprofen, and Krebs-Henseleit buffer (KHB) were purchased from Sigma-Aldrich (St. Louis, MO). Coumarin and midazolam were obtained from Wako Pure Chemical Industries (Osaka, Japan). All other chemicals and solvents were of the highest or analytical grade commercially available.

Generation of mice with humanized livers: The present study was approved by the ethics committee of PhoenixBio Co., Ltd. and the Hiroshima Prefectural Institute of Industrial Science and Technology Ethics Board.

Cryopreserved h-hepatocytes from three donors (4YF, a 4-year-old Caucasian girl; 6YF, a 6-year-old African-American girl; and 2YM, a 2-year-old Caucasian boy) were purchased from BD Biosciences (San Jose, CA). Three (donor 4YF), 17 (donor 6YF), and 4 (donor 2YM) chimeric mice with humanized livers, generated by a method described previously, were used.[1] The concentration of human albumin (hAlb) in the blood of the chimeric mice and the replacement index (RI, the rate of hepatocyte replacement from mouse to human) were well correlated.[1] In the current study, we used 11–15-week-old male and female chimeric mice with approximately 11–14 mg/mL hAlb in mouse blood (RI > 70%); uPA/SCID mice were used as controls.

Isolation of hepatocytes from chimeric mouse liver, SCID mouse liver, and human liver tissue: Hepatocytes were isolated from the 4YF-, 6YF-, and 2YM-chimeric mice using a two-step collagenase perfusion method. The liver was perfused at 38°C for 10 min at 1.5 mL/min with Ca^{2+}-free and Mg^{2+}-free Hanks' balanced salt solution (CMF-HBSS) containing 200 mg/mL ethylene glycol tetraacetic acid (EGTA), 1 mg/mL glucose, 10 mM *N*-2-hydroxyethylpiperazine-*N'*-2-ethanesulfonic acid (HEPES), and 10 μg/mL gentamicin. The perfusion solution was then changed to CMF-HBSS containing 0.05% collagenase (Wako Pure Chemical Industries), 0.6 mg/mL $CaCl_2$, 10 mM HEPES, and 10 μg/mL gentamicin, and perfusion was continued for 17–23 min at 1.5 mL/min. The liver was dissected and transferred to a dish; liver cells were gently disaggregated in the dish with CMF-HBSS containing 10% bovine Alb, 10 mM HEPES, and 10 μg/mL gentamicin. The disaggregated cells were centrifuged three times (50 × *g*, 2 min). The pellet was suspended in medium consisting of Dulbecco's modified Eagle's medium (DMEM), 10% fetal bovine serum (FBS), 20 mM HEPES, 44 mM $NaHCO_3$, and antibiotics (100 IU/mL penicillin G and 100 μg/mL streptomycin). Cell number and viability were assessed using the trypan blue exclusion test.

Normal liver tissues were obtained from the resected liver of nine patients (51-, 53-, and 64-year-old men and a 68-year-old woman for plating efficiency; 54-, 57-, and 75-year-old men for P450 activity; and 55- and 69-year-old women for screening of monoclonal antibodies) after receiving consent prior to surgery, in accordance with the 1975 Declaration of Helsinki. Hepatocytes were isolated via two-step collagenase perfusion and low-speed centrifugation.[1] Aliquots of freshly isolated hepatocytes from four individuals, used for determining plating efficiency, were suspended at $1–2 \times 10^7$ cells/mL/vial in cryopreservation solution (Cellbanker; Juji Field, Inc., Tokyo, Japan), cryopreserved using a program freezer (Kryo-10 Series III; Planer Products Ltd., Sunbury-on-

Thames, Middlesex, UK), and kept in liquid nitrogen. To measure the plating efficiency of the hepatocytes, 4YF-chimeric hepatocytes and hepatocytes from human livers were inoculated onto 13.5-mm Celldesks (Sumitomo Bakelite, Tokyo, Japan) in 24-well plates (BD Biosciences) for 24 h, followed by fixation with ethanol and staining with hematoxylin and eosin. Adhered hepatocytes were counted under the microscope and plating efficiency was calculated by dividing number of adhered cells by the cell number inoculated in a well.

Hepatocytes were isolated from three male uPA (wt/wt)/SCID mice by collagenase perfusion methods.[9] They were used for *in vitro* glucuronidation activity studies.

Purification of h-hepatocytes from total hepatocytes of the chimeric mouse livers: A Fischer 344 rat was immunized intraperitoneally three times (once a week) with 10^7 mouse hepatocytes (m-hepatocytes) of SCID mice as an antigen, and injected with a booster of 2.5×10^7 m-hepatocytes at 3 weeks after the last immunization. Hybridomas were obtained by conventional methods and screened on immunohistochemical sections using m- and h- (from a 55-year-old woman) liver tissues. Frozen h- and m- liver sections were incubated with hybridoma supernatants and fluorescein-labeled anti-rat IgG antibodies (Alexa Fluor 594; Molecular Probes, Eugene, OR). Supernatants from 10 hybridoma clones were reacted with the plasma membrane of m-hepatocytes, but not with h-hepatocytes on the sections. The reactivity of each of the supernatants to the cell surface was determined with a fluorescence-activated cell sorter (FACS) as follows. Isolated m- and h- (69-year-old woman) hepatocytes were incubated with the supernatants and fluorescein isothiocyanate (FITC)-conjugated second antibodies (Alexa Fluor 488; Molecular Probes) and analyzed with a FACS Vantage SE (BD Biosciences) using a 100-μm nozzle. Fluorescence excited at 488 nm was measured through a 530-nm filter (FL1) with 4-decade logarithmic amplification. A hybridoma clone was selected as the clone that produced antibodies reactive to the cell surface of m-hepatocytes, but not h-hepatocytes. The antibody was purified from the culture medium of the hybridoma cells by protein G affinity column or ion exchange chromatography; the antibody was named 66Z.

Isolated h-hepatocytes from chimeric mice were contaminated with m-hepatocytes. To remove the m-hepatocytes, 6YF-hepatocytes isolated from the chimeric mice were incubated with the 66Z antibody, washed with DMEM containing 10% FBS, and incubated with Dynabeads M450-conjugated sheep anti-rat IgG (Dynal Biotech, Milwaukee, WI) in a tube for 30 min on ice. The tube was placed in Dynal MPC-1 (Dynal Biotech) for 1–2 min to remove 66Z-positive ($66Z^+$) m-hepatocytes. Enriched h-hepatocytes were collected as 66Z-negative ($66Z^-$) cells. Aliquots of chimeric hepatocytes from before and after enrichment were incubated with FITC-conjugated 66Z antibodies, and the proportion of $66Z^+$-cells in the h-hepatocytes was determined by FACS.

***In vitro* metabolic study using hepatocytes and microsomes:** For the measurement of the P450 activities of four fresh and five cryopreserved 6YF-chimeric mice, cryopreserved donor cells (6YF), and fresh h-hepatocytes from three individuals, suspended hepatocytes (6×10^4 cells) were incubated in KHB with each of eight substrates specific for seven P450 subtypes (phenacetin for CYP1A2, coumarin for CYP2A6, tolbutamide for CYP2C9, *S*-mephenytoin for CYP2C19, dextromethorphan for CYP2D6, chlorzoxazone for CYP2E1, and midazolam and testosterone for CYP3A) in 96-well plates (BD Biosciences) for 1 or 2 h (**Table 1**). The incubated solution was collected and an equivalent volume of methanol containing 1 μM niflumic acid (internal standard) was added. After centrifugation (10,000 rpm), the supernatant was subjected to liquid chromatography-tandem mass spectrometry (LC-MS/MS) (MDS SCIEX; Applied Biosystems, Foster City, CA). The LC system consisted of an HP 1100 system including a binary pump, an automatic sampler, and a column oven (Agilent Technologies, Waldbronn, Germany), equipped with a Symmetry Shield C18 column (Waters, Tokyo, Japan). The column temperature was 35 °C. The mobile phase was 40% acetonitrile/0.1% formic acid (v/v). The flow rate was 0.3 mL/min. The LC was connected to a PE Sciex API2000 tandem mass spectrometer (Applied Biosystems), operated in positive electrospray ionization mode. The turbo gas was maintained at 550 °C. Nitrogen was used as the nebulizing gas, turbo gas, and curtain gas at 65, 85, and 30 psi, respectively. Parent and/or fragment ions were filtered in the first quadrupole and dissociated in the collision cell using nitrogen as the collision gas. The analytical conditions for each substrate are shown in **Table 2**. The experiments were performed in triplicate per mouse, and the results are expressed as the average value of three mice or humans.

To assess changes in the P450 activities of fresh and cryopreserved 2YM-chimeric hepatocytes during storage at 4 °C for 3 and 6 h, fresh and cryopreserved chimeric hepatocytes were prepared from two 2YM chimeric mice. The isolated hepatocytes from the chimeric mice were purified by isodensity centrifugation (27% Percoll, 7 min, 4 °C) to remove dead hepatocytes. Cells (4×10^5 cells) were incubated in KHB with four different substrates specific for four P450s (phenacetin for CYP1A2, diclofenac for CYP2C9, *S*-mephenytoin for CYP2C19, and midazolam for CYP3A) in 24-well plates (BD Biosciences) for 2 h (**Table 1**). The incubated solution was collected and the concentration of the metabolites was measured by high-performance liquid chromatography (HPLC; Lachome Elite; Hitachi High-Technology Co., Tokyo, Japan). HPLC was performed at

Table 1. Reaction conditions for determination of CYP activities using cells and microsomes for LC-MS/MS and HPLC analysis

Enzymes measured	Enzyme activity	Substrate (concentration, mM)	Metabolite	Cells (LC-MS/MS)	Cells (HPLC)	Microsomes (LC-MS/MS)	
				Incubation time (h)	Incubation time (h)	Buffer*	Incubation time (min)
CYP1A2	Phenacetin *O*-deethylase	Phenacetin (15)	Acetaminophen	2	2	PB	20
CYP2A6	Coumarin 7-hydroxylase	Coumarin (8)	7-Hydroxycoumarin	2	–	TB	20
CYP2C9	Tolbutamide 4-hydroxylase	Tolbutamide (150)	Hydroxytolbutamide	2	–	TB	10
	Diclofenac 4′-hydroxylase	Diclofenac (100)	4-Hydroxydiclofenac	–	2	–	–
CYP2C19	*S*-Mephenytoin 4′-hydroxylase	*S*-Mephenytoin (20)	(±)-4′-Hydroxymephenytoin	2	2	PB	20
CYP2D6	Dextromethorphan *O*-demethylase	Dextromethorphan (8)	Dextrorphan	2	–	PB	20
CYP2E1	Chlorzoxazone 6-hydroxylase	Chlorzoxazone (100)	6-Hydroxychlorzoxazone	2	–	PB	20
CYP3A	Midazolam 1′-hydroxylase	Midazolam (10)	1′-Hydroxymidazolam	1	2	PB	10
	Testosterone 6β-hydroxylase	Testosterone (50)	6β-Hydroxytestosterone	2	–	PB	10

*TB, Tris-HCl buffer (pH 7.5); PB, potassium phosphate buffer (pH 7.4).

Table 2. Analytical parameters of LC-MS/MS for CYP1A2, 2A6, 2C9, 2C19, 2D6, 2E1, and 3A assays

Enzymes measured	Analyte	Mass spectrometer conditions						
		Mode	Declustering potential (eV)	Collision energy (eV)	Entrance potential (eV)	Collision cell exit potential (eV)	Ionspray voltage (V)	Analyte *m/z* transition
CYP1A2	Acetaminophen	Positive	40	25	7	10	5000	152.2→110.3
CYP2A6	7-Hydroxycoumarin	Positive	80	30	7	10	4200	162.8→107.2
CYP2C9	Hydroxytolbutamide	Positive	40	25	7	10	5000	286.9→171.3
CYP2C19	(±)-4′-Hydroxymephenytoin	Positive	80	25	7	10	4200	234.9→150.1
CYP2D6	Dextrorphan	Positive	120	40	7	10	4200	259.0→200.2
CYP2E1	6-Hydroxychlorzoxazone	Negative	−80	−25	−7	−10	−4200	184.1→120.0
CYP3A	6β-Hydroxytestosterone	Positive	60	25	7	10	4200	305.9→270.3
	1′-Hydroxymidazolam	Positive	100	40	7	10	5000	341.6→203.3
Ketoprofen	Ketoprofen	Positive	80	35	7	10	5000	255.5→104.9

a flow rate of 1.0 mL/min using the CAPCELL PAK C18, UG120 (4.6×250 mm, 5 μm; Shiseido, Tokyo, Japan) for CYP1A2 and CYP2C19, Inertsil ODS-3 (4.6×250 mm, 5 μm; GL Sciences Inc., Tokyo, Japan) for CYP2C9, and Xterra RP18 (4.6×150 mm, 5 μm; Waters) for CYP3A. Other analytical conditions are shown in **Table 3**. The measurements were performed in duplicate.

Liver microsomes were prepared from a 6YF-chimeric mouse and control uPA/SCID mice as described previously.[10] They were stored at −80°C until analysis. The protein concentration was determined using a Bradford protein assay kit (Bio-Rad, Hercules, CA), using bovine serum albumin as the standard. Microsomes from a chimeric mouse liver, pooled microsomes of six uPA/SCID mice, and pooled microsomes of 20 human livers (BD Gentest; BD Biosciences) were incubated with the substrates at 37°C for 5 min following incubation with the reduced form of nicotinamide adenine dinucleotide phosphate (NADPH) cofactor solution (3.8 mM β-$NADP^+$, 9.7 mM glucose-6-phosphate, 9.7 mM $MgCl_2$, 1.2 U/mL glucose-6-phosphate dehydrogenase) at 37°C for 10 or 20 min (**Table 1**). The incubated solution was collected and the concentration of the metabolites was measured by LC-MS/MS. The experiments were performed in triplicate per microsome preparation, and the results are expressed as the average value.

Detection of CYP2A6 gene mutations by the Invader assay: CYP2A6 polymorphism was determined by BML, Inc. (Tokyo, Japan). Genomic DNA was isolated from thawed human hepatocytes and the DNA was used

Table 3. Analytical conditions of HPLC for CYP1A2, 2C9, 2C19, and 3A assays

Enzymes measured	Analyte	Internal standard	Injection volume (μL)	Mobile phase			Column temperature (°C)	UV detection (nm)
				Solvent A*	Solvent B	Gradient program, %B (min)		
CYP1A2	Acetaminophen	0.1 μg Caffeine monohydrate	95	50 mM PB (pH 4.0)	Acetonitrile	Isocratic mode (A/B=91/9)	35	245
CYP2C9	4′-Hydroxydiclofenac	0.4 μg Phenacetin	50	0.5% (v/v) AAAS	Methanol containing 0.5% (v/v) acetic acid	40 (0)→90 (30) →90 (35)→40 (36)	50	280
CYP2C19	(±)-4′-Hydroxymephenytoin	0.1 μg Phenobarbital sodium	95	50 mM PB	Acetonitrile	Isocratic mode (A/B=80/20)	35	240
CYP3A	1′-Hydroxymidazolam	0.01 μg Phenacetin	50	10 mM PB (pH 7.4)	Acetonitrile/methanol mixture (7/5, v/v)	30 (0)→30 (5)→60 (17) →60 (25)→30 (26)	40	263

*PB, potassium phosphate buffer; AAAS, acetic acid aqueous solution.

for determining CYP2A6 polymorphism by the Invader assay.[11]

***In vitro* glucuronidation activity study using hepatocytes:** Ketoprofen metabolism was examined using three types of hepatocytes: fresh and cryopreserved 6YF-chimeric hepatocytes, cryopreserved donor cells (6YF), and fresh uPA(wt/wt)/SCID mouse hepatocytes. Hepatocytes (4×10^5 cells) suspended in KHB were plated in 24-well, non-treated plates (BD Biosciences) and incubated at 37°C for 15 min. The cells were treated with 1 μM ketoprofen at 37°C for 3 h. The medium was harvested and aliquots of the medium were incubated at 37°C for 4 h with 0.25 M acetic acid buffer as a solvent control (A) and with 2500 units/mL β-glucuronidase (B). Equivalent 1 N KOH was added into (B) and incubated at 80°C for 3 h (C). After incubation, an equivalent of methanol containing 1 μM niflumic acid (as an internal standard) was added. After centrifugation (10,000 rpm), the supernatant was subjected to LC-MS/MS.

The relevant concentrations can then be obtained:

[Concentration of ketoprofen in (B)] − [Concentration of ketoprofen in (A)] gives [Concentration of ketoprofen-glucuronide].

[Concentration of ketoprofen in (C)] − [Concentration of ketoprofen in (B)] gives [Concentration of transferred ketoprofen-glucuronide].

The transferred ketoprofen is the acyl glucuronide positional isomer, formed by acyl migration, which may be the glucuronide form transferred from ketoprofen-glucuronide during incubation. The experiments were performed in triplicate for a given mouse, and the results are expressed as the average value of three chimeric mice for fresh chimeric hepatocytes, the average of five chimeric mice for cryopreserved hepatocytes, and the average of three uPA(wt/wt)/SCID mice for fresh control mouse hepatocytes.

Statistics: The data were analyzed using Statcel2 (OMS Publishing Inc., Tokorozawa, Japan). Results are expressed as the mean ± SD, and the significance of the difference between two groups was analyzed by Student's *t*-test when data were normally distributed, and by Welch's *t*-test otherwise. $P < 0.05$ was deemed to indicate statistical significance.

Results

Yield, viability, and plating efficiency of isolated h-hepatocytes: Hepatocytes from the 4YF-, 6YF-, and 2YM-donors were transplanted into uPA/SCID mice, and chimeric mice were obtained bearing the respective donor hepatocytes (**Table 4**). The chimeric mice (4YF, 3 mice; 6YF, 17 mice; 2YM, 4 mice) were sacrificed at 54–83 days post-transplantation (**Table 4**). On the day they were sacrificed, blood was collected for the determination of hAlb concentrations (**Table 4**). Hepatocytes were then isolated by the collagenase perfusion method. Numbers (yield) of isolated viable hepatocytes were approximately $2–3 \times 10^7$ cells/mouse (**Table 4**). The viabilities were approximately 60–70% and 50–60% for fresh and cryopreserved chimeric hepatocytes, respectively, without Percoll purification.

The plating efficiency of hepatocytes from the chimeric mice was about 66.6 ± 3.4% (mean ± SD), while those of fresh hepatocytes and cryopreserved hepatocytes from human livers were 34.0 ± 19.3% and 9.3 ± 8.3%, respectively.

Purification of h-hepatocytes isolated from chimeric mice: Chimeric hepatocyte preparations consisted of h- and m-hepatocytes. It was found that 17.3 ± 6.7% of the fresh hepatocytes from 6YF-chimeric mice were $66Z^+$ ($n = 4$; **Table 4**) by FACS analysis. The enriched chimeric hepatocytes were found to be 3.3 ± 1.0% $66Z^+$ (m-hepatocytes; $n = 4$; **Table 4**).

P450 activities of hepatocytes from the chimeric mice: The P450 activities of hepatocytes from 6YF-chi-

Table 4. Hepatocytes used for the experiments

Purpose	Origin	Fresh or cryopreserved	n (sex of host animals or patients)	hAl in mouse blood (mg/mL)	Yield of hepatocytes ($\times 10^7$ cells)	Viability (%)	Ratio of mouse hepatocytes (%)	
							Before purification	After purification
Plating efficiency	Chimeric mouse (4YF)	Fresh	3 (M: 1, F: 2)	11.5±3.6	2.90±2.7/mouse	63.9±6.5	N.D.[*4]	N.D.
	Human liver (51–68-year-old)	Fresh	4 (M: 3, F: 1)	–	0.98±0.4/g liver	87.9±8.2	–	–
		Cryopreserved	4 (M: 3, F: 1)	–	–	56.2±7.5[*5]	–	–
CYP activities	Chimeric mouse (6YF)	Fresh	4[*1] (F)	11.8±0.6	1.78±0.9/mouse	61.8±6.9	17.3±6.7	3.3±1.0
		Cryopreserved	5[*2] (M: 2, F: 3)	12.6±2.1	–	60.5±10.6[*5]	5.8±4.7[*5]	2.1±1.0[*5]
	Human liver (54–75-year-old)	Fresh	3 (M: 3)	–	0.43±0.4/g liver	96.1±2.4	–	–
	Donor cell (6YF)	Cryopreserved	1 (F)	–	–	71.1	–	–
CYP activities at different time points after perfusion or thawing	Chimeric mouse (2YM)	Fresh	2[*3] (F)	11.8	3.05[*5),6)]/mouse	84.8[*5),6)]	N.D.	N.D.
		Cryopreserved	2[*3] (F)	11.8	–	86.4[*5),6)]	N.D.	N.D.
Glucuronide activities	Chimeric mouse (6YF)	Fresh	3 (F)	13.5±2.9	3.24±1.0/mouse	69.8±11.2	9.8±2.0	–
		Cryopreserved	5 (M: 3, F: 2)	13.4±2.4	–	50.7±5.1[*5]	12.5±7.2	–
	Donor cell (6YF)	Cryopreserved	1 (F)	–	–	86.7	–	–
	uPA (wt/wt)/SCID mouse	Fresh	3	–	1.51±0.3/mouse	73.2±4.7	–	–

[*1] Hepatocytes from one of four mice were used for CYP1A2, 2C9, and 3A (testosterone), and those from another were used for CYP2A6, 2C19, 2D6, 2E1, and 3A (midazolam). Hepatocytes from two mice were used for all tested P450s.
[*2] Hepatocytes from one of five mice were used for CYP1A2, 2C9, and 3A (testosterone); those from a second mouse were used for CYP2A6, 2C19, and 2E1; those from a third mouse were used for CYP2C19, 2D6, 3A (midazolam); and those from a fourth mouse were used for tested P450s except for CYP2C19. Those from a fifth mouse were used for all tested P450s.
[*3] Hepatocytes from one of two mice were used for CYP1A2 and 3A, and those from the second mouse were used for CYP2C9 and 2C19.
[*4] Not determined.
[*5] Data after thaw.
[*6] Data after purification with Percoll.

meric mice were determined using eight substrates (**Table 1**). The reactions of P450 activities with all substrates shown in **Table 1** were linear with incubation time. The activities of fresh chimeric hepatocytes were compared with cryopreserved chimeric hepatocytes and cryopreserved donor cells. Three experiments were performed and the means±SD are given in **Figure 1**. CYP1A2, 2C19, and 2D6 activities in fresh chimeric hepatocytes were approximately twice those in cryopreserved cells (**Fig. 1**). CYP2A6, 2C9, 2E1, and 3A activities in fresh chimeric hepatocytes were similar to those of cryopreserved hepatocytes (**Fig. 1**). The activities of cryopreserved donor cells (6YF) were lower than those of cryopreserved 6YF-chimeric hepatocytes in CYP1A2, 2C19, and 3A (midazolam); higher in CYP2A6 and 2E1; and similar in CYP2C9, 2D6, 3A (testosterone; **Fig. 1**). Compared with CYP2A6 activities of two of the three fresh hepatocytes, CYP2A6 activity was extremely low in the chimeric hepatocytes (**Fig. 1**). Interestingly, the Invader assay revealed that donor 6YF had the *1/*4 CYP2A6 polymorphism; livers with the *1/*4 polymorphism in CYP2A6 are known to show low CYP2A6 activity.[12] We concluded that the low CYP2A6 activity was due to the *1/*4 polymorphism of donor 6YF. Three kinds of fresh h-hepatocytes were also examined for P450 activity. One of the three samples did not show CYP1A2 or 2C19 activity. Large individual differences were observed among the three in CYP2A6, 2C9, and 2E1 activities. The activities of CYP1A2, 2C19, 2D6, and 3A in fresh h-hepatocytes were lower than those in fresh chimeric hepatocytes.

We determined changes in the P450 activities of fresh and cryopreserved 2YM-chimeric hepatocytes after Percoll purification during storage at 4°C after isolation and thawing, respectively. CYP1A2, 2C9, 2C19, and 3A activities did not change for up to 6 h after isolation or thawing (**Fig. 2**). CYP1A2, 2C19, and 3A activities were lower in cryopreserved chimeric hepatocytes, and CYP2C9 activity was similar compared to fresh chimeric hepatocytes at 0 h after isolation or thawing (**Fig. 2**). The results were reproducible and are similar to those in **Figure 1**.

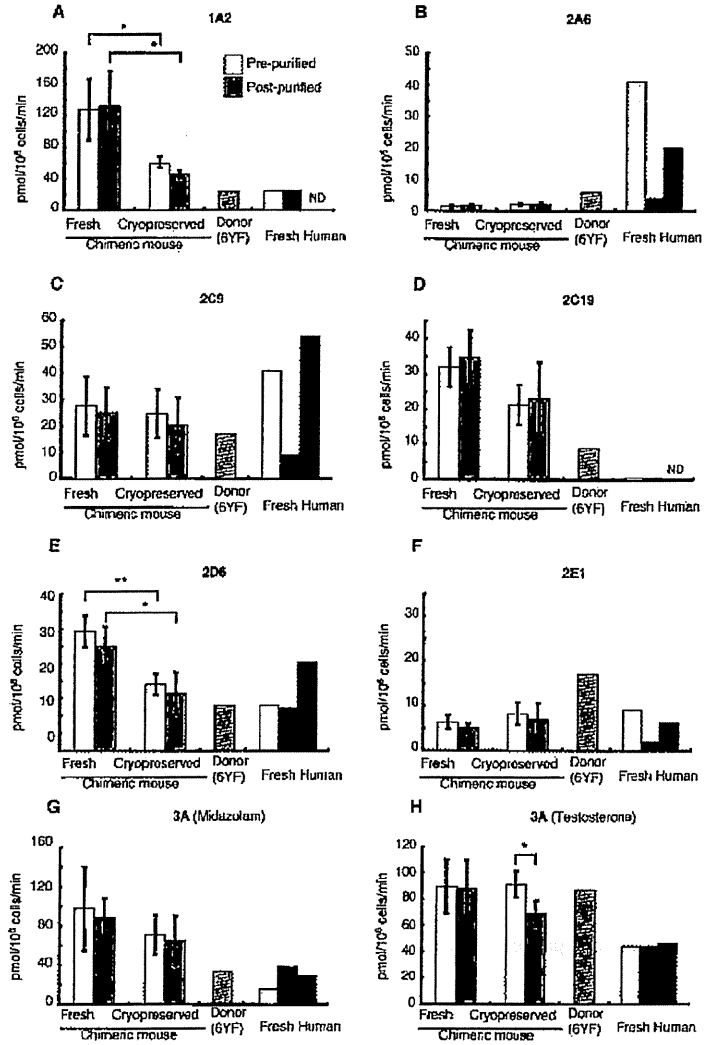

Fig. 1. P450 activities of fresh and cryopreserved chimeric hepatocytes, cryopreserved donor hepatocytes, and fresh h-hepatocytes, determined by LC-MS/MS

Hepatocytes were isolated from 6YF-chimeric mice. Aliquots of the isolated hepatocytes were frozen with a programmed freezer. Aliquots of fresh and thawed cryopreserved chimeric hepatocytes were purified with 66Z antibodies by magnetic sorting. Cryopreserved donor hepatocytes (6YF) for the chimeric mice were thawed. Fresh h-hepatocytes were isolated from resected livers after surgery from three patients. Eight kinds of suspended hepatocytes were incubated with eight substrates specific for seven P450s (Table 1): (A) 1A2, (B) 2A6, (C) 2C9, (D) 2C19, (E) 2D6, (F) 2E1, (G) 3A, midazolam, and (H) 3A, testosterone. The incubated medium was analyzed for each metabolite by LC-MS/MS (Table 2) and the metabolic activity of each P450 is shown as pmol/10^6 cells/min. Data in fresh and cryopreserved chimeric hepatocytes are shown as means ± SD of metabolite concentrations of three different chimeric mice. $^*p<0.05$, $^{**}p<0.01$. ND, not detected.

Contribution of m-hepatocyte contamination in chimeric hepatocytes to P450 activity: The proportions of m-hepatocytes in the fresh chimeric hepatocytes were approximately 17% and 3% before and after purification with 66Z antibodies, respectively, as described above. To determine how the contaminating m-hepatocytes affected P450 activities, we measured P450 activities using liver microsomes from a 6YF-chimeric mouse, pooled host uPA/SCID mice, and pooled human liver microsomes. Except for CYP2D6 and 2E1, P450 activities were similar or lower in uPA/SCID mouse liver microsomes than in human pooled microsomes (**Fig. 3**). Because the activities of CYP2D6 and 2E1 in uPA/SCID mouse liver microsomes were 50–100% higher than in pooled human microsomes (**Fig. 3**), we considered that m-hepatocytes contaminating the chimeric hepatocytes at around 17% might not significantly affect the activities of chimeric hepatocytes. We measured the P450 activity of pre- and post-purified chimeric hepatocytes (6YF) using 66Z antibodies. The purified hepato-

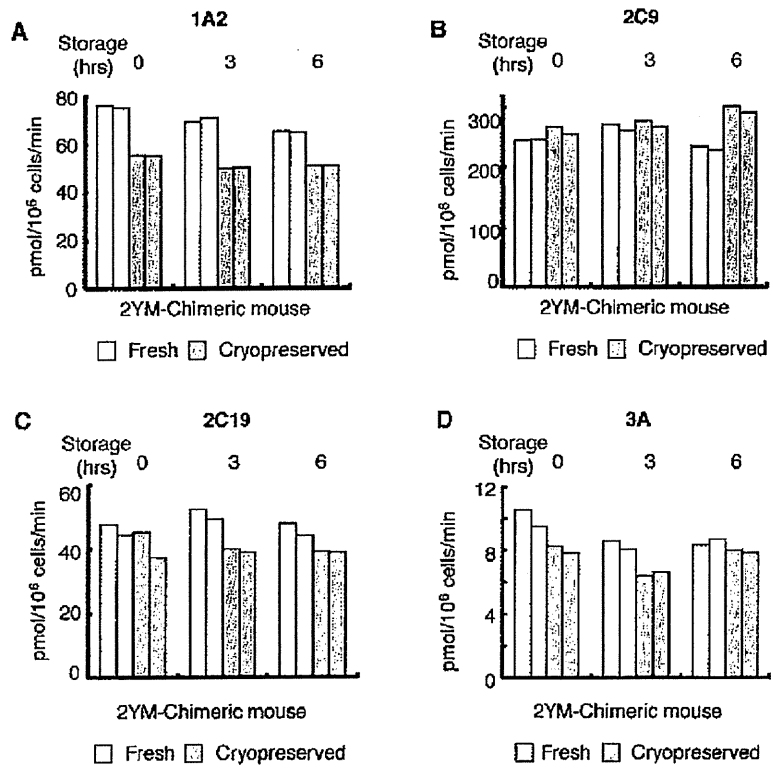

Fig. 2. Time course of P450 activities in fresh and cryopreserved chimeric hepatocytes after isolation or thawing, respectively, as assessed by HPLC

Fresh and cryopreserved 2YM-chimeric hepatocytes were stored after isolation and thawing, respectively, at 4°C for 3 and 6 h. The fresh and cryopreserved chimeric hepatocytes were purified by Percoll isodensity centrifugation after isolation or thawing. Fresh and cryopreserved chimeric hepatocytes, just after purification (0 h) and after storage for 3 h and 6 h, were treated with four substrates specific for four P450s (Table 1): (A) 1A2, (B) 2C9, (C) 2C19, and (D) 3A. The incubated medium was used to analyze each metabolite by HPLC; the metabolic activity of each P450 is shown as pmol/10^6 cells/min (Table 3).

cytes from the chimeric mice showed similar P450 activities to unpurified ones, supporting this suggestion (**Fig. 1**).

Glucuronide conjugation of ketoprofen in chimeric m-hepatocytes: Glucuronide conjugates were detected by *in vitro* metabolic assay for ketoprofen using fresh and cryopreserved hepatocytes from the 6YF-chimeric mouse and cryopreserved donor cells (6YF); however, uPA(wt/wt)/SCID mouse hepatocytes did not show products of UGT activity. The proportion of non-metabolized ketoprofen in fresh chimeric hepatocytes was similar to that in donor cells and lower than that in cryopreserved chimeric hepatocytes (**Fig. 4**). The proportion of ketoprofen-glucuronide in fresh chimeric hepatocytes was significantly higher than that of both cryopreserved chimeric hepatocytes ($P < 0.05$). The transferred ketoprofen-glucuronide levels in fresh chimeric hepatocytes were also higher than those of both cells, but not significantly so (**Fig. 4**). From these results, we suggest that the freeze-thaw procedure decreased cellular glucuronide conjugation activities on drugs such as ketoprofen.

Discussion

Recent studies have revealed that chimeric mice may be a useful model for the examination of drug absorption, distribution, metabolism, and excretion (ADME) and drug interactions via enzyme induction and inhibition *in vivo*.[1,3,4,7,12-14] S-Warfarin has been shown to be metabolized to S-7-hydroxywarfarin, catalyzed by CYP2C9, and is primarily recovered in urine in humans.[15] The mass balance and metabolic disposition of S-warfarin in chimeric mice were found to be similar to reported human data.[14,16] In humans, ketoprofen is primarily metabolized by UGT and converted to ketoprofen glucuronides.[8] When chimeric mice were administered ketoprofen, glucuronide conjugates were detected in their sera and bile.[7] By treatment with typical inducers of P450 (3-methylcholanthrene and rifampicin), human CYP1A and CYP3A4, respectively, were induced in the chimeric mouse liver.[1,3] After treatment with quinidine, a specific inhibitor of human CYP2D6, the area under the curve (AUC) of CYP2D6 metabolites was significantly decreased in the chimeric mice, but not in